

---

TOPICAL SEMINAR  
ON ELECTROMAGNETIC INTERACTIONS

ICTP, Trieste, 21-26 June 1971.

---

International Atomic Energy Agency  
and  
United Nations Educational Scientific and Cultural Organization

INTERNATIONAL CENTRE FOR THEORETICAL PHYSICS

PHOTOPRODUCTION OF VECTOR MESONS  
(EXPERIMENTAL) \*

P. Söding

Deutsches Elektronen-Synchrotron DESY, Hamburg, Fed. Rep. Germany.

MIRAMARE - TRIESTE

October 1971


\* An invited talk presented at the above Seminar.

1. Introduction

As the quantum numbers of the vector mesons equal those of the photon, it is not surprising that vector meson photoproduction is related to hadronic elastic scattering. More precisely, the current-field identity<sup>1</sup>

$$-j_\mu(x) = \frac{m_\rho^2}{2\gamma_\rho} \rho_\mu^0(x) + \frac{m_\omega^2}{2\gamma_\omega} \omega_\mu(x) + \frac{m_\phi^2}{2\gamma_\phi} \phi_\mu(x) + \dots ?$$

(where  $j_\mu$  is the hadronic electromagnetic current;  $\rho_\mu^0$ ,  $\omega_\mu$  and  $\phi_\mu$  are the vector meson fields,  $m_V$  the vector meson masses and  $\gamma_V$  the coupling parameters) leads us to consider the photon-hadron interaction to be mediated by the vector mesons, with a direct photon-vector meson coupling



$$-\frac{em^2_V}{2\gamma_V} \quad (e^2/4\pi = 1/137)$$

In the limit of unbroken SU(3), ideal  $\omega\phi$  mixing, and zero mixing with other possible vector states, the couplings are in the famous ratio

$$\frac{1}{\gamma_\rho} : \frac{1}{\gamma_\omega} : \frac{1}{\gamma_\phi} = 3 : 1 : (-\sqrt{2});$$

this is changed somewhat by symmetry-breaking<sup>2</sup> (see section 9).

The data on photoproduction of vector mesons allow some rather direct tests of the vector-meson dominance model of the electromagnetic current.<sup>2</sup> They may also reveal some of the general properties of hadronic processes. On first sight vector meson photoproduction at high energies is a particularly pure example of a diffractive production process. Helicity conservation has already been discovered here and has suggested itself as perhaps a new principle for certain types of reactions.<sup>3</sup>

On closer examination however the data do not always follow our often generalizing expectations. And vector dominance, although doing surprisingly well in some respects, apparently fails in others.

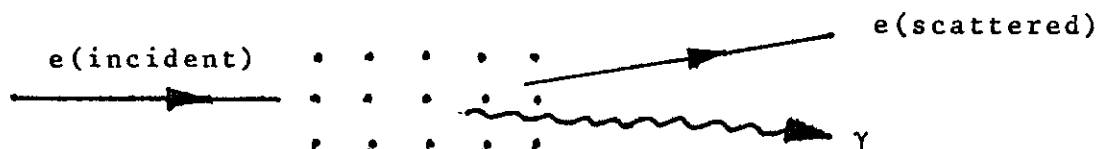
This report will start with a brief description of methods to polarize photons (section 2), followed by a discussion of the polarization properties of  $\rho^0$ ,  $\omega$  and  $\phi$  photoproduction (sections 3 - 5). Next we consider the cross sections for vector meson photoproduction on protons (section 6) and their implications for the vector-dominance model (section 7). This is followed by a discussion of photoproduction on deuterons (section 8) and complex nuclei (section 9), which allows further tests of vector dominance. We then turn to the photoproduction phases (section 10) and end with a brief discussion on photoproduction of heavy mesons (section 11).

We will concentrate in this presentation on some of the newer and (supposedly) more important experimental results. No effort is made on completeness, for which the many good recent reviews offer an excellent excuse.<sup>4-11</sup>

## 2. Polarized Photon Beams

### a) Coherent bremsstrahlung from a diamond monocrystal.<sup>12,13</sup>

In the bremsstrahlung of high-energy electrons on the atoms of a regular lattice, one observes a strong enhancement if the momentum transfer coincides with a vector of the reciprocal lattice. The photons under this condition turn out to be linearly

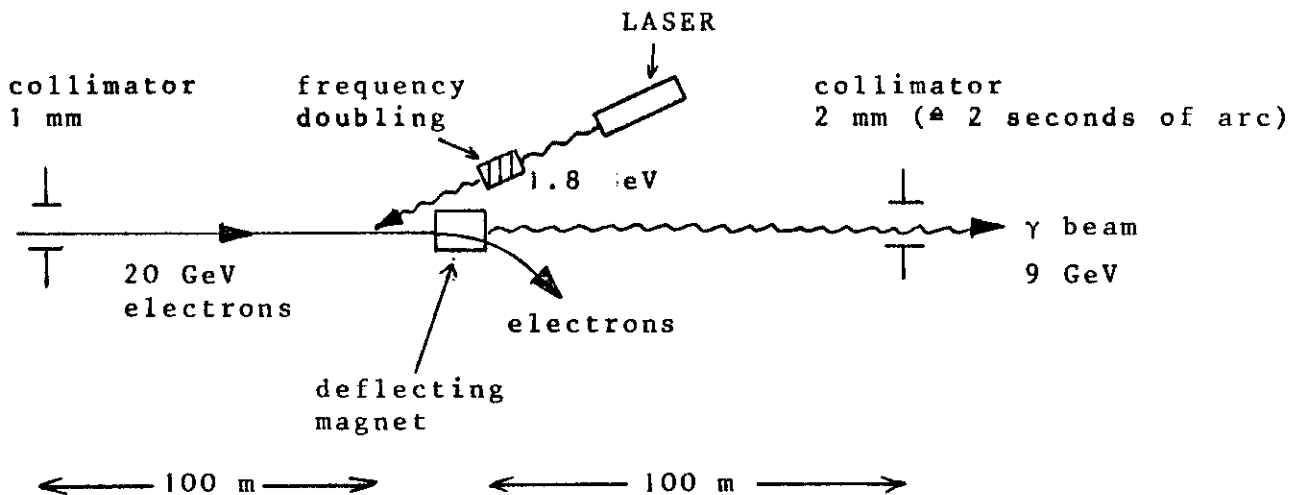


polarized, with a polarization of up to ~70 %. This method to polarize photons has been used in vector-meson production experiments at Cornell, DESY, and SLAC. Rather intense beams can

be produced. Large polarization is however achieved only at  $E_{\gamma} \leq \frac{1}{2}E_{\text{incident}}$ , which limits the usable photon energy  $E_{\gamma}$  to  $\leq 5$  GeV at Cornell and  $\leq 3.5$  GeV at DESY. Furthermore there is a large, flat, unpolarized photon background extending up to  $E_{\gamma}^{\text{max}} = E_{\text{incident}}$ .

b) "Acceleration" of polarized light.<sup>14,15</sup>

Light from a laser is Compton-scattered under  $\approx 180^{\circ}$  on high-energy electrons. The backscattered photons thereby achieve high energy in the laboratory system. As Compton scattering is a two-body process, the final-state photon energy  $E_{\gamma}$  depends only on the scattering angle. One can therefore obtain a nearly monochromatic photon beam by sufficiently collimating the electron and photon beams. The polarization (linear or circular) of the laser light is essentially retained in the scattering process. This method has been used to study vector meson photoproduction by linear



polarized photons of  $E_{\gamma} = 2.8$  GeV, 4.7 GeV and 9.3 GeV at SLAC.<sup>16-19</sup> The polarization was 94 % at 2.8 and 4.7 GeV, and 77 % at 9.3 GeV. The small intensity and short pulse length of the photon beams so obtained limit their use to bubble chamber experiments.

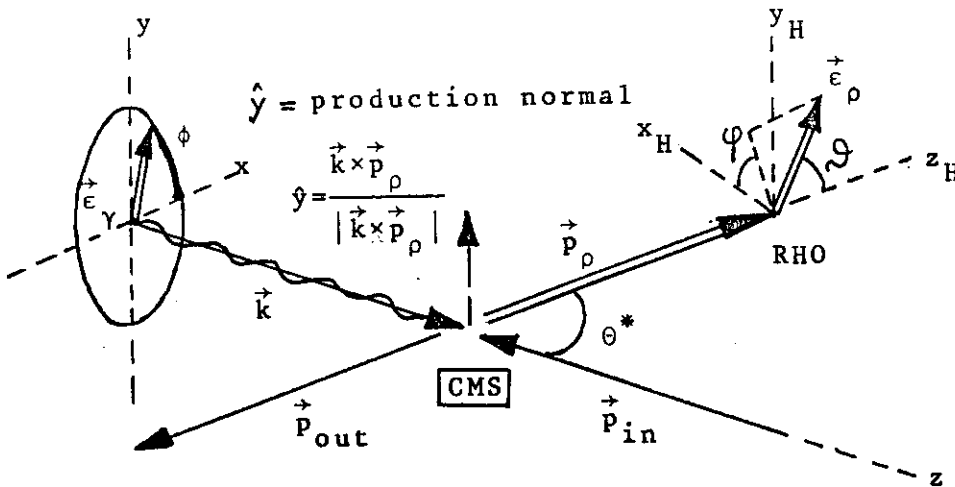
A comparison of the spectra of a coherent bremsstrahlung beam used recently at Cornell<sup>20</sup>, with the one from the laser Compton scattering<sup>17</sup>, is shown in Fig. 1.

c) Photon absorption in highly oriented graphite<sup>21</sup>.

If a beam of high-energy photons is passed through oriented single crystals of graphite, photons with different directions of their polarization vector will be absorbed differently. This is due to the fact that the cross section for coherent  $e^+e^-$  pair production depends on the relative orientation of the polarization vector and the crystal axis. In a recent experiment at Cornell, a polarization of 6 % was achieved at a beam energy of 9 GeV. Higher degrees of polarization are expected when  $E_\gamma$  becomes higher, so that the method could be useful at the new accelerators.

3. Polarization Properties of the Reaction  $\gamma p \rightarrow \rho^0 p$

Assume the incident photon beam to be linearly polarized, with degree of polarization  $P_\gamma$ . Let  $\phi$  be the angle between the photon



polarization vector  $\vec{\epsilon}_\gamma$  and the production plane. Then the helicity

density matrix<sup>22</sup> of the  $\rho^0$  meson depends on  $\phi$  in the following way:

$$\rho_{\lambda\lambda'} = \rho_{\lambda\lambda'}^{(0)} - P_\gamma \cos 2\phi \rho_{\lambda\lambda'}^{(1)} - P_\gamma \sin 2\phi \rho_{\lambda\lambda'}^{(2)} .$$

The  $\phi$  dependence cannot be more complicated due to the fact that the spin of the photon is 1.  $\rho_{\lambda\lambda'}^{(0)}$  is the density matrix for the unpolarized case. It turns out<sup>23</sup> that from observation of the  $\rho^0$  decay angular distribution  $W(\cos\theta, \varphi; \phi)$  using linearly polarized photons, one can determine a total of 9 independent (real or imaginary parts of) elements of the density matrices  $\rho_{\lambda\lambda'}^{(0)}$ ,  $\rho_{\lambda\lambda'}^{(1)}$  and  $\rho_{\lambda\lambda'}^{(2)}$ . Therefore one gets 10 times as much information (differential cross section plus 9 density matrix elements) as from a mere differential cross section measurement.

The determination of the 9 density matrix elements has been done only in the bubble chamber, since one needs the full (or at least a large part of the) decay angular distribution  $W(\cos\theta, \varphi; \phi)$  to separate the various matrix elements.

We do not want to discuss here the general expression for the decay angular distribution  $W(\cos\theta, \varphi; \phi)$  in terms of the density matrix. We mention only two simple properties. We take  $\theta$  and  $\varphi$  to be the polar and azimuthal angles of the  $\pi^+$  from the  $\rho^0 \rightarrow \pi^+ \pi^-$  decay, measured in the  $\rho^0$  rest system in the s-channel helicity frame ( $x_H, y_H, z_H$ ). This frame is defined by a  $z_H$  axis parallel to  $-\vec{p}_{out}$  and a  $y_H$  axis parallel to the normal to the production plane (see sketch above). The polarization vector  $\vec{\epsilon}_\rho$  of the  $\rho^0$  meson is parallel to the relative momentum  $\vec{p}_{\pi^+} - \vec{p}_{\pi^-}$  of the decay pions in the  $\rho^0$  rest system.

The first property has to do with the question of helicity conservation. We can have the helicities

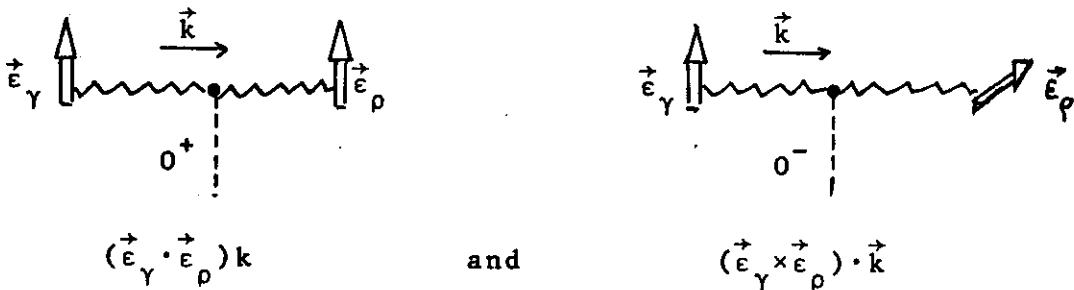
$$\lambda_\gamma = \pm 1 \quad \text{for the photon,} \quad \lambda_\rho = 0, \pm 1 \quad \text{for the } \rho^0 .$$

The question arises: Are there "helicity flip" transitions into the  $\lambda_\rho = 0$  state? This can be answered from the  $\cos\theta$  distribution alone, even with unpolarized photons, since

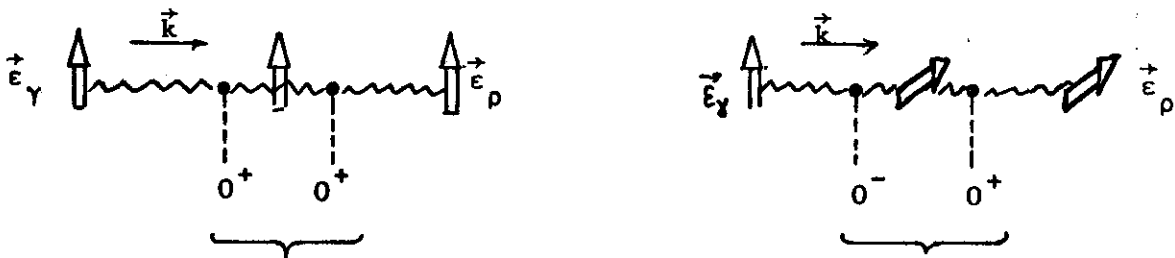
$$W(\cos\theta) = \begin{cases} \text{const} \left| Y_{1}^{\pm 1} \right|^2 = \text{const} \cdot \sin^2\theta & \text{for } \lambda_{\rho} = \begin{cases} \pm 1 \\ 0 \end{cases} \\ \text{const} \left| Y_{1}^{0} \right|^2 = \text{const} \cdot \cos^2\theta & \end{cases}$$

in the s-channel helicity frame.

The second property relates the exchange of natural vs. unnatural spin-parity in the t-channel, with the correlation of the photon and the  $\rho^0$  polarization planes. To make it plausible we use a simple mnemonic. Imagine the photon - rho meson transition at small cms angles  $\theta^*$ , with exchange of a  $J^P = 0^+$  or  $0^-$  object. The matrix elements are<sup>24</sup>



(e.g. for  $0^-$  remember the perpendicular polarization planes of the photons from  $\pi^0$  decay). For exchange of higher spins, the mnemonic is



can combine to total  
exchange of  $J^P = 0^+, 1^-, 2^+ \dots$   
(= natural series)

can combine to total  
exchange of  $J^P = 0^-, 1^+, 2^- \dots$   
(= unnatural series)

Let  $\Psi (= \varphi - \phi)$  be the angle between  $\vec{\epsilon}_\gamma$  and the projection of  $\vec{\epsilon}_\rho$  onto a plane perpendicular to  $\vec{k}$ . Then we have from the square of the matrix elements

$$W(\Psi) \propto \cos^2 \Psi \quad (\text{natural exchange})$$

$$W(\Psi) \propto \sin^2 \Psi \quad (\text{unnatural exchange}).$$

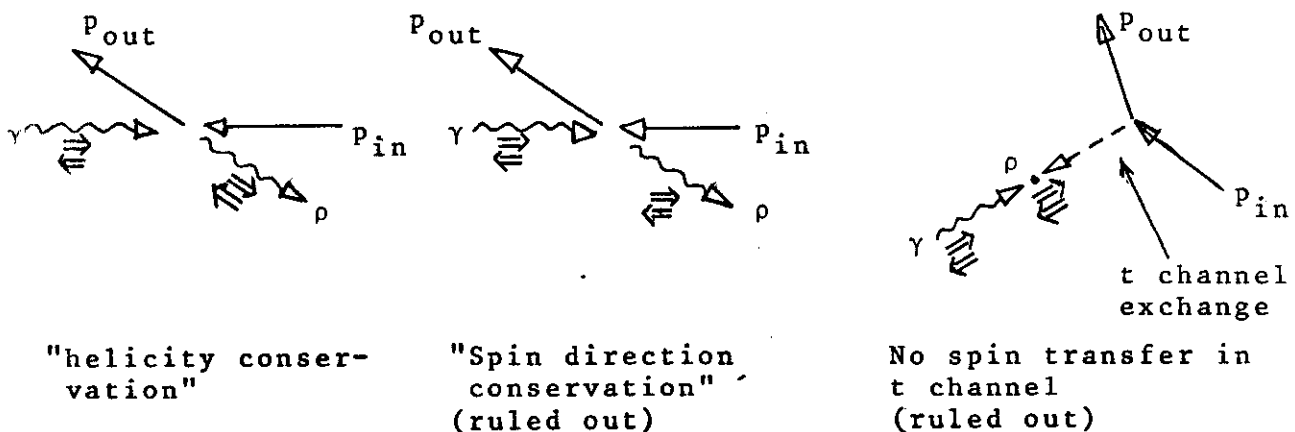
At large cms production angles  $\theta^*$  it turns out still to be true that for natural (unnatural) exchange the  $\Psi$  distribution peaks at 0 and 180 deg (90 and 270 deg)<sup>23</sup>.

Experimental evidence for the tendency of the  $\rho^0$  in the reaction  $\gamma p \rightarrow \rho^0 p$  to emerge with helicities  $\lambda_\rho = \pm 1$  like the photon, was first reported by the ABBHBM bubble chamber collaboration with data obtained at DESY<sup>25</sup>. The most convincing evidence is provided by the bubble chamber data of the SLAC-Berkeley-Tufts Collaboration<sup>17,19</sup>. In Fig. 2 we show some of their recent unpublished data on the reaction  $\gamma p \rightarrow \pi^+ \pi^- p$  at 9.3 GeV, obtained with the Compton backscattered polarized photon beam<sup>19</sup>. The left part of the figure shows the Dalitz plot  $M_{\pi^+ \pi^-}^2$  vs.  $M_{p \pi^+}^2$ . One sees the  $\rho^0$  and the  $\Delta^{++}(1236)$  bands, and perhaps an indication of  $\Delta^0(1236)$  production. Note that there is some additional background, outside the  $\rho^0$  and  $\Delta(1236)$  bands. On the right hand side of Fig. 2 is part of the Chew-Low plot,  $M_{\pi^+ \pi^-}^2$  vs.  $|t|$ , where  $t = (p_\gamma - p_{\pi^+ \pi^-})^2$  is the square of the four-momentum transfer from the photon to the mesons. Small  $|t|$  are strongly preferred. The slope of the  $t$  distribution is seen to vary with  $M_{\pi^+ \pi^-}^2$ , or put differently, the form of the  $M_{\pi^+ \pi^-}$  mass distribution is seen to change with  $t$ . This causes difficulties in determining the  $\rho^0$  production cross section since obviously it cannot have a simple Breit-Wigner resonance form.

The decay angular distributions of the  $\pi^+ \pi^-$  system for events in the  $\rho^0$  mass region and for small momentum transfer ( $|t| < 0.4 \text{ GeV}^2$ ) from this experiment are shown in Fig. 3. The polar angle distribution is compatible with  $\sin^2 \mathcal{J}$ , consistent with complete helicity conservation at the  $\gamma\rho$  vertex. The  $\Psi$  data show clear evidence for overwhelming natural  $J^P$  exchange. The distribution is not expected to go exactly to zero at  $90^\circ$  and  $270^\circ$  since the photons were only 77 % polarized.



The most concise way to visualize the apparent conservation of helicity in  $\rho^0$  photoproduction is presented in Fig. 4, also from the SLAC-Berkeley-Tufts experiment<sup>19</sup>. Consider a coordinate frame, in the rest system of the  $\rho^0$ , in which the  $\rho^0$  density matrix most closely resembles that of the initial photon (i.e. pure transverse polarization, same polarization plane). Then let  $\beta$  be the angle of rotation, around the normal to the production plane, that transforms the s-channel helicity frame into this minimum-flip system. It is seen in Fig. 4 that at 9.3 GeV,  $\beta$  is not far from zero up to  $|t| = 0.8 \text{ GeV}^2$ . Also shown in Fig. 4 are the angles of rotation from the helicity frame<sup>22</sup> into the Adair frame<sup>26</sup> (Curve A), and into the Gottfried-Jackson frame<sup>27</sup> (Curve GJ). These frames differ from the s-channel helicity frame only by a rotation around the normal to the production plane. The helicity frame has its z axis parallel to  $\vec{p}_\rho$  in the cms, the Adair frame parallel to  $\vec{p}_\gamma$  in the cms, and the Gottfried-Jackson frame parallel to  $\vec{p}_\gamma$  in the  $\rho^0$  rest system; the y axes are always perpendicular to the production plane. Zero flip in the Adair system would imply "spin direction conservation" while zero flip in the Gottfried-Jackson frame would hold if no spin was exchanged in the t channel:



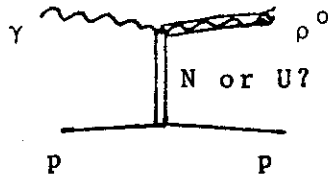
One sees from Fig. 4 that the latter two possibilities are definitely ruled out for  $|t| < 0.8 \text{ GeV}^2$ . Contrast this with the situation in the reactions, also believed to be diffractive,

$$\pi^\pm p \rightarrow A_1^\pm p, \quad K^\pm p \rightarrow Q^\pm p$$

where the data are more or less consistent with zero flip in the Gottfried-Jackson frame, and incompatible with s-channel helicity conservation<sup>28</sup>. The reason for this difference in behavior is not clear. These reactions differ however from photoproduction of neutral vector mesons in two respects:

- (i) The  $J^P$  quantum numbers of the bosonic system change in the reaction.
- (ii) The  $A_1$  and  $Q$  may not be genuine resonances. - In any case we conclude from Fig. 4 that for  $\rho^0$  photoproduction, helicity conservation at the  $\gamma\rho$  vertex may hold up to  $|t| \sim 1 \text{ GeV}^2$  at high energy.

We now discuss more quantitatively the question of natural vs. unnatural spin-parity exchange in the reaction  $\gamma p \rightarrow \rho^0 p$ :



We define the

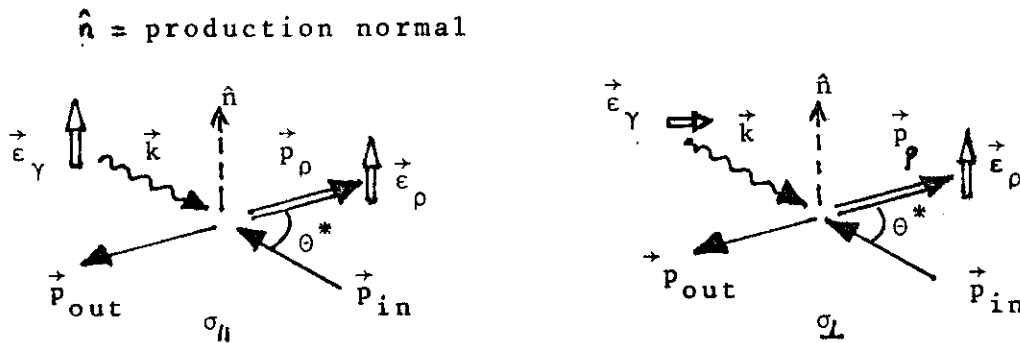
"parity asymmetry" 
$$P_\sigma = \frac{\sigma_N - \sigma_U}{\sigma_N + \sigma_U} \approx 2 \rho_{1,-1}^{(1)} - \rho_{00}^{(1)}$$

(to leading order in  $E_\gamma$ <sup>23,29</sup>), and the

"asymmetry ratio"  $\Sigma = \frac{\sigma_{||} - \sigma_{\perp}}{\sigma_{||} + \sigma_{\perp}}$

$$= \frac{(\rho_{11}^{(0)} + \rho_{1-1}^{(0)})^N - (\rho_{11}^{(0)} + \rho_{1-1}^{(0)})^U}{(\rho_{11}^{(0)} + \rho_{1-1}^{(0)})^N + (\rho_{11}^{(0)} + \rho_{1-1}^{(0)})^U} = \frac{\rho_{11}^{(1)} + \rho_{1-1}^{(1)}}{\rho_{11}^{(0)} + \rho_{1-1}^{(0)}}$$

Here, the superscripts N and U mean natural and unnatural  $J^P$  exchange;  $\sigma_{||}(\sigma_{\perp})$  is the cross section for the case where the  $\rho$  polarization vector  $\vec{\epsilon}_{\rho}$  is orthogonal to the production plane and the  $\gamma$  polarization vector  $\vec{\epsilon}_{\gamma}$  parallel (orthogonal) to  $\vec{\epsilon}_{\rho}$ , as illustrated below:



Loosely speaking  $\Sigma$  is the relative contribution of natural vs. unnatural  $J^P$ -exchange, to the production of helicity  $\pm 1$  vector meson states. For diffraction production one expects  $P_{\sigma} = \Sigma = 1$ .

Figure 5 shows the measured values<sup>17,30,31</sup> of  $\Sigma$  as a function of the photon energy  $E_{\gamma}$ . They are very nearly equal to +1 in the whole energy range measured, from 1.7 to 5 GeV. Note that  $\Sigma$  can take values between -1 and +1. Figure 6 shows  $P_{\sigma}$  at 9.3 GeV as a function of  $|t|$ <sup>19</sup>. It is seen to be compatible with 1 in the whole measured  $|t|$  range, from 0 up to 0.8 GeV<sup>2</sup>.

As the leading unnatural  $J^P$  exchange contribution to  $\rho^0$  photoproduction we may expect pion exchange. From SU(3) symmetry and the quark model one has  $\Gamma_{\rho\pi\gamma} = \frac{1}{9} \Gamma_{\omega\pi\gamma} = 0.13$  MeV.

Using this for the  $\rho\pi\gamma$  coupling one finds the pion exchange contribution to  $\rho^0$  photoproduction as given in Table I. It is seen to be just compatible, within the experimental errors, with the unnatural t-channel exchange contributions found in the SLAC-Berkeley-Tufts experiments<sup>17,19</sup>.

TABLE I. Unnatural Exchange Contribution<sup>17,19</sup>, and expected Pion Exchange Contribution<sup>32</sup>, to  $\sigma(\gamma p \rightarrow \rho^0 p)$

$E_\gamma$ (GeV)  t  range (GeV <sup>2</sup> )	2.8 <1	4.7 <1	9.3 .05 <  t  <  t  <sub>MAX</sub>
$\sigma^U / (\sigma^N + \sigma^U)$	(3.1 ± 3.1)%	(-1.1 ± 2.8)%	(-0.5 ± 4.5)%
$\sigma_\pi / (\sigma^N + \sigma^U)$	2 %	0.8 %	0.2 %

An interesting question is whether p-wave  $\pi^+\pi^-$ -systems produced by natural exchange and with helicity conservation, are also seen outside the  $\rho^0$  mass region. Figure 7 shows  $\rho_{00}^{(0)}$ ,  $\rho_{1-1}^{(1)}$  and  $P_\sigma$  as a function of the  $\pi^+\pi^-$  mass, determined from the data under the assumption that the  $\pi^+\pi^-$  system is in a pure p-wave state<sup>17</sup>. In the  $\rho^0$  region,

$\rho_{00}^{(0)}$  = degree of longitudinal polarization of the  $\pi^+\pi^-$  system, = 1

$\rho_{1-1}^{(1)}$  = correlation term between  $\lambda_\rho = \pm 1$  states for linearly polarized photons (necessary to give linearly polarized  $\rho$ 's), =  $\frac{1}{2}$

$P_\sigma$  = parity asymmetry = 1

but outside of the  $\rho^0$  mass region these quantities change drastically. This is clear evidence for a background behaving quite different from the  $\rho^0$ . It does not come unexpected of course, since (see Fig. 2) part of the higher-mass  $\pi^+\pi^-$  states (however not all) are decay products of  $\Delta(1236)$ .

To summarize, we may state that the polarization properties found in the reaction  $\gamma p \rightarrow \rho^0 p$  are compatible with s-channel helicity conservation at the bosonic vertex, and with natural  $J^P$  t-channel exchange. The contribution to the cross section of unnatural exchange and of helicity flip in the photon- $\rho^0$  transition is quite small up to  $|t| \sim 0.8 \text{ GeV}^2$  at 9 GeV.\* A large nucleon helicity flip contribution cannot yet be excluded. As the most important t-channel exchanges we may expect exchange of  $P$ ,  $P'$ , and  $A_2$ .

#### 4. Polarization Properties of the Reaction $\gamma p \rightarrow \omega p$

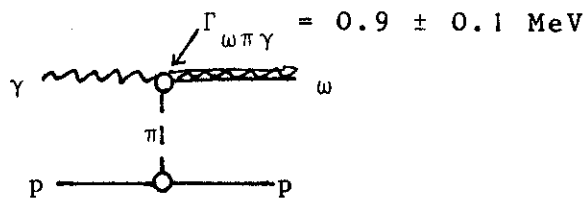
This reaction has been studied with linearly polarized photons also by the SLAC-Berkeley-Tufts Collaboration<sup>18,19</sup>. They detect the decay  $\omega \rightarrow \pi^+ \pi^- \pi^0$  in the bubble chamber. The formalism is the same as for  $\gamma p \rightarrow \rho^0 p$ , with the difference that the  $\omega$  polarization vector is given by the normal  $\hat{n}$  to the three-pion plane in the  $\omega$  rest system,  $\vec{\epsilon}_\omega = \hat{n}$ , because the decay matrix element (apart from form factors) is  $\vec{M}_\omega = \vec{p}_0 \times (\vec{p}_+ - \vec{p}_-)$ .

Figure 8 shows the decay angular distributions of the  $\omega$  in the helicity system, and the parity asymmetry  $P_\sigma$ , at 2.8, 4.7 and 9.3 GeV<sup>18,19</sup>. At all three energies,  $W(\cos \theta)$  does not quite agree with the form  $\sin^2 \theta$  expected for s-channel helicity conservation.  $P_\sigma$  seems to be strongly energy-dependent, rising from

---

\* It has been remarked recently<sup>33,34</sup> that for any exchange with well-defined naturality (natural or unnatural), only the s-channel helicity conserving amplitudes can be  $\neq 0$  in the exact forward direction, due to angular momentum and parity conservation. This does not imply that our conclusion on helicity conservation reduces to a triviality. Thus spin-flip in the Adair system, which has precisely the same kinematical zeros  $((\sin \theta^*) |m_\gamma + m_p - m_\rho - m_{p'}|)$  in forward direction, actually is clearly observed (see Fig. 4). Still, some of the helicity flip amplitudes may be substantial although their contribution to the cross section remains small, due to the small size of the kinematical factors multiplying these amplitudes.

0 at 3 GeV to  $\approx 1$  at 9 GeV. A separation into natural and unnatural t-channel  $J^P$  exchange parts of the total  $\omega$  photoproduction cross section is shown in Fig. 9. The natural exchange part (open circles) is seen to be only weakly energy-dependent, the energy-dependence being consistent with that for  $\rho^0$  photoproduction (dashed curve). This suggests diffraction to be the dominant mechanism. At 9 GeV,  $\sigma^N \approx 2 \mu\text{b}$ . On the other hand the unnatural exchange cross section drops like  $E_\gamma^{-2}$ . In fact it is quantitatively consistent with pion exchange with Benecke-Dürr



form factors<sup>35,36</sup> (full curve in Fig. 9).

### 5. Polarization Properties of the Reaction $\gamma p \rightarrow \phi p$

This reaction has been measured by several groups, all of which detected the  $\phi \rightarrow K^+ K^-$  decay. The  $\phi$  decay angular distribution  $W(\cos\theta)$  in the helicity system has been looked at by the DESY-MIT group<sup>37</sup> (using however a nucleus as target), and the ABBHMM bubble chamber collaboration<sup>25</sup>, both finding it consistent with  $\sin^2\theta$  as expected for s-channel helicity conservation. These experiments suffered however either from a restricted  $\theta$ -range available, or from small statistical accuracy.

The only published results with linearly polarized photons are from the Cornell group<sup>20</sup>. They detected  $\phi$ 's produced near the forward direction at an average photon energy of 5.7 GeV. For the asymmetry ratio (defined in Section 3) they found

$$\Sigma = \begin{cases} 0.94 \pm 0.06 & \text{(on a C nucleus target)} \\ 0.53 \pm 0.15 & \text{(on a H target)} \end{cases}$$

The large deviation of  $\Sigma$  on the H target from the expected value of 1 would mean a sizable nondiffractive (unnatural exchange) component,  $d\sigma_{\perp}/d\sigma_{\parallel} = 0.30 \pm 0.12$ . The Cornell group is presently looking into the question of "inelastic"  $\phi$  production perhaps contaminating their measurements<sup>38</sup>. (For example, the ABBHBM group had found a cross section  $\sigma(\gamma p \rightarrow \pi^+ \pi^- \phi p) = 0.6 \pm 0.2 \mu\text{b}$  at  $E_{\gamma} \sim 5 \text{ GeV}$ .<sup>40</sup>) Should the small measured value of  $\Sigma$  be confirmed it would seem rather a puzzle since the reaction  $\gamma p \rightarrow \phi p$  is thought, motivated mainly by the quark picture, to be a particularly pure example of a reaction proceeding by P exchange<sup>41,42</sup>. Candidates for unnatural  $J^P$  exchange are  $\pi$  and  $\eta$ ; however with the recent Orsay values  $\Gamma_{\phi\pi\gamma} = .0076 \pm .0032 \text{ MeV}$  and  $\Gamma_{\phi\eta\gamma} = .077 \pm .023 \text{ MeV}$ <sup>39</sup>, and taking account of the interference between the two exchanges, one computes a rather small contribution of unnatural exchange such that the resulting asymmetry  $\Sigma$  would still be  $\geq 0.92$  at 5.7 GeV and small  $\Theta^*$ <sup>32</sup>.

#### 6. Cross Sections of the Reactions $\gamma p \rightarrow V^0 p$

In the determination of cross sections for  $\rho^0$ ,  $\omega$  and  $\phi$  photoproduction one meets several difficulties. Part of them is of a purely instrumental nature. Thus, bubble and streamer chamber experiments usually miss events with  $|t| \leq 0.02 \text{ GeV}^2$ , and some losses can occur up to  $|t| = 0.05 \text{ GeV}^2$ . In most counter and spark chamber experiments only the decay products of the vector mesons are detected; since the photon beams are not monochromatic one has the problem of separating off the "inelastic background"\* from reactions like<sup>43</sup>

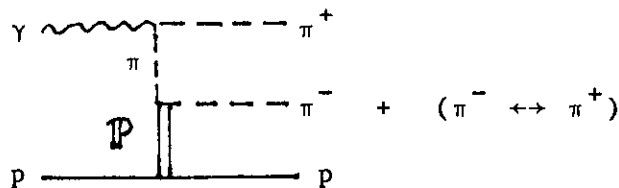
$$\gamma p \rightarrow V^0 p + n\pi \quad (n \geq 1).$$

\* Inelastic background contributions to  $\rho^0$  and  $\phi$  photoproduction have been recently measured for specific kinematic conditions by the Cornell group, who have added a p recoil hodoscope to their forward pair spectrometer<sup>38</sup>. They found these contributions to be of the order of (5 - 25)% for  $E_{\gamma} \approx 8.5 \text{ GeV}$  and  $|t| < 0.5 \text{ GeV}^2$ .

Moreover in some of these experiments one has limited decay angular acceptance, which makes it necessary to assume, say, helicity conservation at small  $t$  for  $\rho^0$  and  $\phi$  in order to deduce cross sections summed over all decay directions<sup>44</sup>. Both difficulties were absent in the SLAC missing mass-type experiment where only the recoil proton is measured<sup>45</sup>; however here the mass resolution was not sufficient to separate  $\omega$  from  $\rho^0$ .

In addition, the experimenters also face problems of a more fundamental nature when they try to determine V meson production cross sections. We list only a few of them.

(i) Background subtraction and interpretation. As we saw from Fig. 2, in the  $M_{\pi^+\pi^-}$  distribution from the reaction  $\gamma p \rightarrow \pi^+\pi^-p$  there is, apart from the background due to  $\Delta^{++}(1236)$  and  $\Delta^0(1236)$  production, some additional background outside of and (probably) underneath the  $\rho^0$  peak. The nature and precise size of this background is not known. Usually one assumes for it either a phase space distribution, or a distribution as given by the Drell diagrams:<sup>46</sup>



Such amplitudes can interfere with  $\rho^0$  production<sup>47,48</sup>. They have parts where the  $\pi^+\pi^-$  system is in a p-wave state. Then the question arises whether taking the p-wave as background is double-counting<sup>49-51</sup>. This has not been resolved in a completely satisfactory way yet<sup>51-53</sup>.

(ii) Problems with the shape of wide resonances. A resonance like the  $\rho^0$  may have its apparent shape modified by a  $M_{\pi^+\pi^-}$  dependence of the production mechanism<sup>52,54</sup>. Remember that we saw in Fig. 2 that the shape of the  $\rho^0$  peak changed with  $t$ . Even if this production dependence were known, we still don't know



the width  $\Gamma(M_{\pi\pi})$  at large  $M_{\pi\pi}$ . Therefore although one can quite well measure the cross section

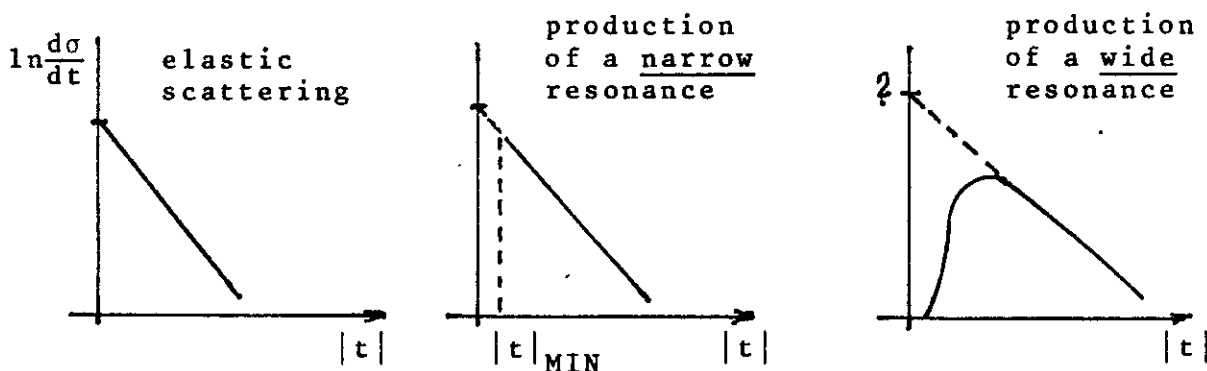
$$\left. \frac{d\sigma}{dM_{\pi\pi}} \right|_{M_{\pi\pi} = m_\rho}$$

at the peak of the  $\rho$ , large uncertainties enter in the determination of

$$\sigma_\rho = \int dM_{\pi\pi} \frac{d\sigma}{dM_{\pi\pi}}$$

The present uncertainty of  $\pm 20$  MeV on the width of the  $\rho$  <sup>55</sup> alone already can cause a cross section error of  $\pm 15$  %.

(iii) Extrapolation of  $\frac{d\sigma}{dt}$  to  $t = 0$ . (This is mainly a problem for bubble and streamer chamber experiments, while in spark chamber experiments on  $H_2$  targets at  $E_\gamma \geq 7$  GeV one was essentially able to measure the  $t = 0$  differential  $\rho^0$  cross sections.) For elastic scattering,  $\frac{d\sigma}{dt}$  behaves typically like an exponential at small  $|t|$ . A similar  $t$  dependence may be expected for diffractive production of a narrow resonance, except that  $|t|_{\text{MIN}} \neq 0$ . But for a wide resonance like the  $\rho$ ,  $|t|_{\text{MIN}}$  depends on the mass, resulting in a more complicated  $t$  dependence of the cross section:



The extrapolation then becomes ambiguous. In some experiments one has effectively corrected the measured  $\frac{d\sigma}{dt}$  values, at fixed

photon energy, to zero width by a factor

$$\frac{d\sigma_{\Gamma \rightarrow 0}}{d\sigma_{\text{exp}}} = \frac{\int dM_{\pi\pi}^2 \delta(M_{\pi\pi}^2 - m_\rho^2) d\sigma(M_{\pi\pi}^2)}{\int dM_{\pi\pi}^2 \text{BW}(M_{\pi\pi}^2) d\sigma(M_{\pi\pi}^2)}$$

(where  $\text{BW}(M_{\pi\pi}^2) = \sin^2 \delta(M_{\pi\pi}) / (\pi m_\rho \Gamma(M_{\pi\pi}))$  is the Breit-Wigner function and  $\delta(M_{\pi\pi})$  the p-wave phase shift), and then extrapolated the values so corrected. Alternatively one may determine  $\frac{d\sigma}{d\Omega^*}$  as a function of the cms angle  $\theta^*$ , convert this into  $\frac{d\sigma}{dt}$  using a central  $\rho$  mass, and extrapolate. In addition to such ambiguities there is the question of whether to include a  $t^2$  term in the extrapolation of  $\ln \frac{d\sigma}{dt}$ . Inclusion of a quadratic term tends to give larger  $\left. \frac{d\sigma}{dt} \right|_{t=0}$  for  $\rho^0$  photoproduction but this term is not really warranted by the data.

From all these difficulties it follows that the determination of  $\rho^0$  photoproduction cross sections is model-dependent, with uncertainties of  $\pm 15\%$  to be expected at finite  $t$ , and perhaps even larger uncertainties at  $|t| \rightarrow 0$ .

After these preliminaries we show in Fig. 10 the results of the differential cross section measurements for the reaction  $\gamma p \rightarrow \rho^0 p$ , obtained in the SLAC missing mass experiment at  $E_\gamma = 5.5 - 18 \text{ GeV}$ <sup>45</sup>. The curves are calculated from the vector-dominance and additive quark-model relation<sup>56</sup>

$$T_{\gamma p \rightarrow \rho^0 p}(s, t) = \frac{e}{2\gamma_\rho} T_{\rho^0 p \rightarrow \rho^0 p} = \frac{e}{2\gamma_\rho} \frac{1}{2} [T_{\pi^+ p \rightarrow \pi^+ p} + T_{\pi^- p \rightarrow \pi^- p}] ,$$

assuming the amplitudes  $T$  to have equal phase, taking  $\frac{d\sigma}{dt} \propto |T|^2$ , and adjusting the one parameter  $\gamma_\rho$ . The authors obtain  $\gamma_\rho^2/4\pi = 0.61$  as an average over the whole energy range. The success of this fit shows that the  $s$  and  $t$  dependence of the  $\rho^0$  photoproduction cross section agrees well with that of elastic pion-nucleon scattering<sup>57</sup>.

The extrapolated forward differential  $\rho^0$  production cross section from this and from several other experiments<sup>17,19,25,58-62</sup> are compiled in Fig. 11. From what has been said it is clear that one cannot expect consistency among all these values. As a general

tendency we note a decrease of the forward cross section up to  $E_\gamma \sim 6$  GeV. For  $E_\gamma \geq 5$  GeV we have

$$\left. \frac{d\sigma}{dt} \right|_{t=0} \approx (80 - 135) \mu\text{b GeV}^{-2}.$$

Within the present errors no indication for s-channel resonance structure at the lower energies is apparent. One has probably to look in the backward direction in order to be more sensitive to resonant amplitudes.

From fits of the form

$$\frac{d\sigma}{dt} = \left. \frac{d\sigma}{dt} \right|_{t=0} \exp(A_\rho t)$$

to the differential  $\rho^0$  production cross sections one obtains slopes in the range of

$$A_\rho = (6 - 9) \text{ GeV}^{-2}$$

at  $E_\gamma \geq 4$  GeV. The integrated total  $\rho^0$  production cross section behaves as<sup>32</sup>

$$\sigma_\rho \approx \frac{e^2}{4\gamma_\rho^2} \frac{1}{2} (\sigma_{\pi^+p}^{el} + \sigma_{\pi^-p}^{el}) \sim E_\gamma^{-0.4} \quad (E_\gamma \geq 3 \text{ GeV})$$

(with  $\gamma_\rho^2/4\pi \sim 0.7$ ), i.e. it is weakly energy-dependent.

We thus see that  $\rho^0$  photoproduction behaves much like hadronic diffraction scattering, as expected from the vector-dominance model. From the weak  $E_\gamma$  dependence we infer that  $\mathbb{P}$  exchange is the dominant t-channel contribution.

The determination of  $\omega$  photoproduction cross sections does not suffer from the large systematic uncertainties described, due to the smaller width of the  $\omega$ . E.g. from Fig. 12 which shows typical  $\rho^0$ ,  $\omega$  and  $\phi$  mass peaks from photoproduction experiments, it is evident that background subtraction under the  $\omega$  is not really problematic. On the other hand, the statistical errors are relatively large since one has to rely on bubble and streamer chamber experiments, counter/spark chamber experiments having problems with background from missing pions.

A compilation of differential  $\omega$  production cross sections from various experiments in the 2 - 8 GeV energy range, from a recent SLAC-Rehovoth paper<sup>63</sup>, is shown in Fig. 13. These cross sections are seen to decrease much stronger with increasing energy than the  $\rho^0$  production differential cross sections (Fig. 10). The curves in Fig. 13 are from a model<sup>63</sup> in which the cross section is expressed as a sum of a diffractive term (whose behavior is assumed identical with that of the  $\rho^0$  production cross sections of the same group<sup>62</sup>) and a pion exchange term with absorptive corrections<sup>64</sup>. The amount of the diffractive contribution is fitted to the data, mainly exploiting the different energy dependence of diffraction and pion exchange. The diffractive part comes out to be  $\sigma_{\omega, \text{diff}} \approx 1.5 \pm 0.3 \mu\text{b}$ , not inconsistent with the natural exchange contributions as determined in the polarized beam experiment of the SLAC-Berkeley-Tufts Collaboration<sup>18</sup> (see Fig. 9 and associated discussion). The SBT Collaboration has also separated the natural and unnatural exchange contributions in the differential  $\omega$  production cross section<sup>18,19</sup>. For the natural  $J^P$  part they find

$$\left. \frac{d\sigma^N}{dt} \right|_{t=0} = \begin{cases} (12.4 \pm 4.2) \mu\text{b GeV}^{-2} & \text{(at 2.8 GeV)} \\ (13.9 \pm 3.8) & \text{(at 4.7 GeV)} \\ (10.6 \pm 2.2) & \text{(at 9.3 GeV)} \end{cases}$$

and a slope of

$$A_{\omega}^N = (6 - 8) \text{GeV}^{-2} .$$

Turning now to cross sections for the reaction  $\gamma p \rightarrow \phi p$ , we show in Fig. 14 a compilation of  $\frac{d\sigma}{dt}$  data at photon energies of 2.5 - 12 GeV<sup>25,37,45</sup>, taken from a recent Cornell paper<sup>65</sup>. The curve is a fit to the Cornell 8 - 9 GeV data;\*

\* These data<sup>65</sup> contain, like probably some of the other  $\phi$  data, contributions from "inelastic"  $\phi$  production reactions like  $\gamma p \rightarrow \phi \pi p$ . After subtraction of this background (see footnote on p. 14) the Cornell group<sup>38</sup> obtained the revised values  $d\sigma/dt|_{t=0} = (2.85 \pm 0.2) \mu\text{b GeV}^{-2}$  and  $A_{\phi} = (5.4 \pm 0.3) \text{GeV}^{-2}$ .

it gives

$$\left. \frac{d\sigma}{dt} \right|_{t=0} = (3.4 \pm 0.2) \mu\text{b GeV}^{-2}$$

and

$$A_{\phi} = (4.7 \pm 0.2) \text{ GeV}^{-2} .$$

There is certainly no drastic variation of the  $\phi$  cross section with  $E_{\gamma}$ ; however, it appears from the SLAC 11.5 GeV data<sup>45</sup> in Fig. 14 that the differential cross section may fall slightly with  $E_{\gamma}$  at the higher energies. The SLAC group has tried a fit to their  $\phi$  data similar to the one described before for their  $\rho^0$  data, using

$$T_{\gamma p \rightarrow \phi p}(s, t) = \frac{e}{2\gamma_{\phi}} T_{\phi p \rightarrow \phi p} = \frac{e}{2\gamma_{\phi}} \left[ T_{K^+ p \rightarrow K^+ p} + T_{K^- p \rightarrow K^- p} - T_{\pi^- p \rightarrow \pi^- p} \right]$$

from vector dominance and the additive quark model<sup>45,56</sup>. It turned out that although the  $t$  dependence agreed reasonably with the model prediction, it was not possible to fit the data at all energies with the same value of  $\gamma_{\phi}^2/4\pi$ . The  $\phi$  cross sections decreased stronger with increasing  $E_{\gamma}$  than the quark model prediction from  $K^+ p$ ,  $K^- p$  and  $\pi^- p$  cross sections<sup>57</sup>. This energy dependence is also indicated in the total cross section for the reaction  $\gamma p \rightarrow \phi p$  shown in Fig. 15<sup>25,38,45,66</sup>. (Note, however, that the SLAC experiment<sup>45</sup> has only data at  $|t| > 0.3 \text{ GeV}^2$  and therefore detects only about 1/4 of the  $\phi$ 's produced.)

7. Test of the Vector Dominance Model

With the data on  $\rho^0$ ,  $\omega$  and  $\phi$  photoproduction discussed we can test the following relation:<sup>67</sup>

$$\begin{aligned}
 \sigma_{\text{tot}}(\gamma p) &= \sqrt{16\pi} \quad \text{Im} \quad \begin{array}{c} \gamma \text{ wavy} \\ \text{---} \text{---} \text{---} \\ \text{p} \text{---} \text{---} \text{---} \text{p} \\ t=0 \end{array} && \text{(optical theorem)} \\
 &= \sqrt{16\pi} \sum_V \text{Im} \quad \begin{array}{c} \gamma \text{ wavy} \\ \text{---} \text{---} \text{---} \\ \text{---} \text{---} \text{---} \\ \text{---} \text{---} \text{---} \\ \text{---} \text{---} \text{---} \\ t=0 \end{array} && \text{(vector dominance)} \\
 &= \sqrt{16\pi} \sum_V \frac{e}{2\gamma_V} \text{Im} \quad \begin{array}{c} \gamma \text{ wavy} \\ \text{---} \text{---} \text{---} \\ \text{---} \text{---} \text{---} \\ \text{---} \text{---} \text{---} \\ \text{---} \text{---} \text{---} \\ t=0 \end{array} && \\
 &= \sqrt{16\pi} \sum_V \sqrt{\frac{e^2}{4\gamma_V^2} \frac{d\sigma^{\text{Im, trans}}}{dt}(\gamma p \rightarrow V^0 p) \Big|_{t=0}}
 \end{aligned}$$

As an estimate of the imaginary parts of the amplitudes for production of transversely polarized vector mesons (with no spin flip on either vertex) we use the square roots of  $d\sigma^N/dt$  (note that e.g. the pion exchange amplitude vanishes at  $t = 0$ ). We take  $\gamma_V$  from the Orsay storage ring experiment<sup>68</sup> on  $e^+e^- \rightarrow \rho, \omega, \phi$ :

$$\gamma_\rho^2/4\pi = 0.64 \pm 0.06, \quad \gamma_\omega^2/4\pi = 4.8 \pm 0.5, \quad \gamma_\phi^2/4\pi = 2.75 \pm 0.22$$

(Note that the value for  $\gamma_\rho^2/4\pi$  agrees with the one obtained by Anderson et al<sup>45</sup> from the vector dominance and quark model relation of p. 17.) Using photoproduction data in the  $E_\gamma = (8 - 9)$  GeV energy region (see section 6) we then have the following contributions to the vector-dominance sum:

vector meson	$\frac{d\sigma}{dt} \Big _{t=0}^{\text{Im,trans}}$	contribution to $\sigma_{\text{tot}}(\gamma p)$
$\rho^0$	80 - 115 $\mu\text{b GeV}^{-2}$	67 - 80 $\mu\text{b}$
$\omega$	11 $\mu\text{b GeV}^{-2}$	9 $\mu\text{b}$
$\phi$	3 $\mu\text{b GeV}^{-2}$	7 $\mu\text{b}$
		sum 83 - 96 $\mu\text{b}$

The total photon-proton cross section<sup>69</sup> at this energy is 120  $\mu\text{b}$ , so that a considerable part of the cross section remains unaccounted for. If we insist on saturating  $\sigma_{\text{tot}}(\gamma p)$  with the  $\rho$ ,  $\omega$  and  $\phi$  contributions, then we have to decrease the values of  $\gamma_V$  (which here apply to the photon mass shell,  $k^2 = 0$ ) relative to the Orsay values (which are for  $k^2 = m_V^2$ ). For the  $\rho$  coupling this leads to

$$\frac{\gamma_{\rho}^2}{4\pi} = 0.26 - 0.38 .$$

The two values for  $\gamma_{\rho}^2/4\pi$  would agree better if the value of  $d\sigma/dt|_{t=0}$  for  $\rho^0$  photoproduction was larger (e.g., as obtained by quadratic extrapolation to  $t = 0$ ). Our neglect of the real parts of the  $\gamma p \rightarrow V^0 p$  amplitudes (see section 10) is not responsible for the discrepancy; for example a real part of the natural-exchange  $\rho^0$  forward production amplitude of 20 % would only reduce the value of  $\gamma_{\rho}^2/4\pi$  by 4 %.

A similar result is obtained if one compares the square root of the differential elastic (Compton) scattering cross section  $\frac{d\sigma}{dt}(\gamma p \rightarrow \gamma p)$ , with an analogous sum over  $\left[ \frac{d\sigma}{dt}(\gamma p \rightarrow V^0 p) \right]^{1/2}$  at finite  $t$ , assuming the phases are all equal. The slopes of  $d\sigma/dt$  are compatible within their relatively large errors, but the same discrepancy in the magnitude occurs as we found for the  $t = 0$  amplitude. (This is discussed in the talk on Compton scattering and total cross sections by Professor M. Deutsch.)

We mention some of the obvious possible reasons for the discrepancy:

- (i) The coupling constants  $\gamma_V$  may depend on  $k^2$ .

- (ii) The amplitude for the reaction  $\gamma p \rightarrow V^0 p$  may depend strongly on the mass of the vector meson produced.
- (iii) There may exist additional hadronic vector states (so that on the right hand side of the vector-dominance relation, the sum runs over more states than just the  $\rho^0$ ,  $\omega$  and  $\phi$ ). See Section 11.
- (iv) There may be an additional "direct" interaction of the photon with the hadrons, outside the framework of the vector-dominance assumption.

As we will discuss in sections 8 and 9, vector dominance seems to correctly relate  $\rho^0$  photoproduction with  $\rho^0$  elastic scattering by nucleons, with a coupling constant in agreement with the Orsay value of  $\gamma_{\rho}^2/4\pi = 0.64$ . This suggests that (i) and (ii) are not the principal reasons for its failure in the present case. On the other hand, we note that the vector dominance relation between single pion photoproduction and vector meson production by pions<sup>2</sup> tends to give similarly small values of  $\gamma_{\rho}^2/4\pi$  as we have obtained here from  $\sigma_{\text{tot}}(\gamma p)$  and vector meson photoproduction.

## 8. Vector Meson Photoproduction on the Deuteron

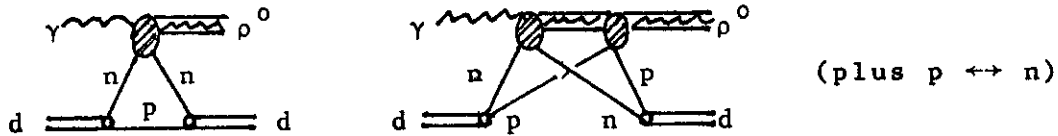
We now consider the reaction

$$\gamma d \rightarrow V^0 d$$

i.e. no break-up of the d. (Such reactions are also called "coherent".) We have  $I = 0$  in the t channel. There are only a few experiments on coherent  $V^0$  production in which the presence of the d in the final state was actually detected.

One of these experiments is the missing-mass experiment done at SLAC, in which only the d was measured<sup>70</sup>. The results for  $d\sigma/dt$  from this experiment are shown in Fig. 16. They cover a  $|t|$  range of 0.15 - 1.4  $\text{GeV}^2$  at 6, 12 and 18 GeV incident photon energy. At  $|t| < 0.4 \text{ GeV}^2$  one finds a very steep slope, corresponding to the d size. Then, a break appears, followed by a much smaller slope. This shows beautifully the regions of single and double scattering in the deuteron<sup>71</sup>. The diagrams for single and double scattering are the following:





Double scattering dominates at larger  $|t|$ , while the single scattering cross section falls with  $|t|$  essentially like the square  $F^2(\frac{|t|}{4})$  of the  $d$  form factor.

If we consider for a moment the double-scattering term, we see that as the intermediate propagating particle the  $\rho^0$  is dominating, while  $\omega$  and  $\phi$  are strongly suppressed. This is due to the fact that we must have  $I = 1$  exchange in both scatterings if we are to have it in one scattering, because only isovector photons can contribute to the overall process. Therefore, double scattering is determined by a product of amplitudes for  $\gamma N \rightarrow \rho^0 N$  and for  $\rho^0 N \rightarrow \rho^0 N$  elastic scattering, and thus provides the chance to observe  $\rho^0 N$  scattering in a rather "clean" and direct way. Also, the real parts of these amplitudes enter only quadratically, so that the results are not sensitive to uncertainties in the real parts (in contrast to the situation with complex nuclei, see section 9).

The curves in Fig. 16 are from a fit to the double scattering region ( $|t| = 0.7 - 1.4 \text{ GeV}^2$ ), with  $d\sigma/dt$  for  $\gamma N \rightarrow \rho^0 N$  taken from the proton data of the same group<sup>45</sup>. By the fit one can then determine some of the parameters of  $\rho^0 N$  elastic scattering; in particular,

$$\sigma_{\rho^0 N} = 28 \pm 2 \text{ mb} \quad (\text{slightly decreasing between 6 and 18 GeV})$$

$$\rho^0 N \text{ slope} \approx \pi^- p \text{ slope}$$

is found. The  $\rho^0 N$  cross section "measured" in this way is reasonably consistent with the additive quark model<sup>56</sup> value of about 25 mb (also slightly decreasing between 6 and 18 GeV); the values deduced from  $\rho^0$  photoproduction on complex nuclei (see Section 9) also agree within errors with this value. With the

results from this experiment one can test the vector dominance model in a finite  $t$  region, using the relation

$$\frac{d\sigma}{dt}(\gamma N \rightarrow \rho^0 N) = \left(\frac{e}{2\gamma_\rho}\right)^2 \frac{d\sigma}{dt}(\rho^0 N \rightarrow \rho^0 N) .$$

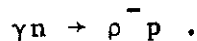
The authors obtain

$$\frac{\gamma_\rho^2}{4\pi} = 0.68 \pm 0.13 ,$$

similar to the Orsay value and to the values deduced from complex nucleus experiments (Section 9). The fit of Fig. 16 also agrees with the data in the single scattering region at small  $|t|$ , which shows that the assumption of  $d\sigma/dt(\gamma n \rightarrow \rho^0 n)$  to be equal to  $d\sigma/dt(\gamma p \rightarrow \rho^0 p)$  does not lead to contradictions.

At smaller  $|t|$  than reached by the SLAC experiment, data have been supplied from the DESY and the SLAC 40" bubble chambers<sup>72,73</sup>. Fig. 17 shows results<sup>72</sup> for  $d\sigma/dt$  in  $|t| = 0.04 - 0.2 \text{ GeV}^2$  at  $E_\gamma = 1.8 - 5.3 \text{ GeV}$ . ( $|t| = 0.04$  is the smallest  $|t|$  value at which the  $d$  can be safely identified in the bubble chamber.)  $d\sigma/dt$  has a slope of about  $\Lambda \approx 25 \text{ GeV}^{-2}$  in this  $t$  region. Here we are definitely in the domain dominated by single scattering. The curves are absolute predictions from the single plus the small double scattering diagrams, using  $\sigma_{\rho^0 N} = \frac{1}{2}(\sigma_{\pi^+ p} + \sigma_{\pi^- p})$  from the quark model for the calculation of the latter (but the result is not sensitive to  $\sigma_{\rho^0 N}$  at these small  $|t|$ ). The essential assumption made in the calculation is that  $\rho^0$  production on single nucleons proceeds entirely by  $I = 0$  exchange, so that the  $p$  and  $n$  amplitudes are identical. Of course, here in single scattering, one can have only  $I = 0$  exchange anyway. But one calculates it under the assumption that the  $I = 0$  exchange part of  $\gamma N \rightarrow \rho^0 N$  is identical with the measured  $\gamma p \rightarrow \rho^0 p$  cross section. From the nice agreement seen in Fig. 17 it follows that the  $I = 1$  exchange contributions to  $\rho^0$  photoproduction on single nucleons cannot be very large. We mention in passing that the data on  $\gamma d \rightarrow \rho^0 d$  for  $|t| < 0.2 \text{ GeV}^2$  are found to be compatible with helicity conservation<sup>72,73</sup>.

A somewhat more sensitive but experimentally difficult test on  $I = 1$  exchange is provided by a measurement of the reaction



Possible exchanges are  $\pi$ ,  $\rho$  and  $A_2$ :

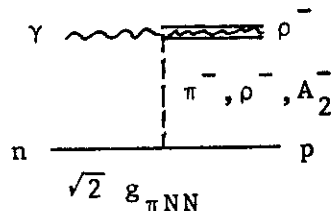
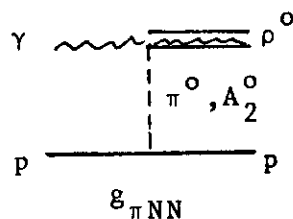


Fig. 18 shows the data from the ABBHBM bubble chamber experiment at DESY<sup>74</sup>. The large errors shown are due to the difficulties stemming from the d target and the presence of a  $\pi^0$  in the final state, from  $\rho^-$  decay. Nevertheless this gives evidence that for  $3.5 \text{ GeV} < E_\gamma < 5.3 \text{ GeV}$  we have  $\sigma_{\rho^-} \leq 1.5 \text{ } \mu\text{b}$ .

Comparing this with the  $I = 1$  exchange diagram for  $\rho^0$  production (note the Clebsch-Gordan factor of  $\sqrt{2}$  vs. 1 at the



nucleon vertex) this suggests\* that

$$\frac{\sigma_{I=1 \text{ exchange}}}{\sigma_{I=0 \text{ exchange}}} < 0.05 \quad \text{for } \gamma N \rightarrow \rho^0 N$$

(which still allows 20 %  $I = 1$  contribution in amplitude).

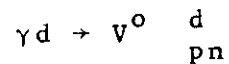
It appears remarkable that also in the low-energy (s-channel resonance) region,  $\sigma_{\rho^-}$  is much smaller than  $\sigma_{\rho^0}$ , as is apparent from Fig. 18.

First data on coherent  $\omega$  photoproduction,  $\gamma d \rightarrow \omega d$ , have been recently shown by the Weizmann group<sup>73</sup>. Within rather large

\*This is not rigorous since although  $\pi$  and  $A_2$  exchanges do not interfere at high energies, the  $A_2$  and  $\rho$  exchanges could interfere destructively in  $\rho^-$  production.

statistical uncertainties they find their data on the ratio of the  $\rho^0$  to  $\omega$  coherent forward production cross sections at  $E_\gamma = 4.3$  GeV to be consistent with the value 9, expected from vector-dominance plus unbroken SU(3) plus the additive quark model.

In addition to the experiments mentioned, spark chamber measurements of the reactions



(i.e. summing over d breakup and non-breakup reactions) have been made for the  $\rho^0$  at Cornell<sup>59,75</sup> and at SLAC<sup>60</sup>, for the  $\omega$  by the Rochester group at Cornell<sup>76</sup>, and for the  $\phi$  at Cornell<sup>65</sup>. In these experiments the  $t$  distributions were measured at energies in the 5 - 16 GeV range, detecting only the decay products of the vector mesons. From their different slopes (roughly  $d\sigma/dt \propto (d\sigma/dt)_{\text{single nucleon}} \times F^2(\frac{|t|}{4})$  for the non-breakup ("coherent") part, and much flatter for the breakup reaction, according to Glauber theory<sup>71</sup>) one can separate the differential cross section into "coherent" and "incoherent" (breakup) parts. For  $|t| \rightarrow |t|_{\text{MIN}}$  the incoherent part becomes relatively small. There may be inelastic coherent background (reactions like  $\gamma d \rightarrow \pi^0 V^0 d$ ) but estimates show this to be small at small  $|t|$ , due to the larger  $|t|_{\text{MIN}}$ . From Glauber theory<sup>71</sup>, taking account of double scattering effects, one predicts values of

$$\frac{d\sigma/dt(\gamma d \rightarrow V^0 d)}{d\sigma/dt(\gamma p \rightarrow V^0 p)} \Big|_{t=0} \approx 3.6 - 3.9$$

(depending on the type of vector meson and the energy) if one assumes that  $\gamma p \rightarrow V^0 p$  is pure  $I = 0$  exchange. This prediction is generally found to agree with the extrapolated  $\rho^0$  and  $\phi$  data for energies above 6.5 GeV, within the experimental uncertainties on the ratio of about  $\pm 0.2$ . Between 4 and 6 GeV for  $\rho^0$  mesons, however, the Cornell d/p ratios are significantly smaller than the prediction with pure  $I = 0$  exchange, indicating an  $I = 1$

exchange amplitude of size ~15 % of the magnitude of the total amplitude for  $\rho^0$  production on the nucleon<sup>75</sup>.

It is interesting to check the vector-dominance relation of section 7 with the extrapolated coherent d cross sections, since isovector exchange amplitudes are absent here. In the reactions on single nucleons these amplitudes might be suspected to cause trouble for the vector-dominance comparison by contributing real parts and/or longitudinal polarization of the vector mesons. With the Orsay coupling constants (see p.21) and photo-production data in the (6-8) GeV energy region, we have (assuming zero real parts and zero helicity flip in the forward direction):

vector meson	$\left. \frac{d\sigma}{dt} \right _{t=0} (\gamma d \rightarrow V^0 d)$	contribution to $\sigma_{tot}(\gamma d)$
$\rho^0$	390 $\mu\text{b GeV}^{-2}$	148 $\mu\text{b}$
$\omega$	-36 $\mu\text{b GeV}^{-2}$ *	-17 $\mu\text{b}$
$\phi$	10 $\mu\text{b GeV}^{-2}$	12 $\mu\text{b}$
		sum 177 $\mu\text{b}$

This is to be compared with the measured total cross section  $\sigma_{tot}(\gamma d) \approx 230 \mu\text{b}$ <sup>69,77</sup>. Saturating  $\sigma_{tot}(\gamma d)$  with the  $\rho$ ,  $\omega$  and  $\phi$  vector-dominance contributions would require a value of

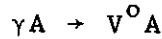
$$\frac{\gamma_{\rho}^2}{4\pi} = 0.35 \pm 0.06 .$$

We thus find a similar difficulty with the vector-dominance model as in  $\gamma p$  reactions (section 7).

\* This value is estimated by extrapolating the closure fit to the Rochester data<sup>76</sup> towards  $t = 0$ . It agrees with the coherent forward cross section quoted in ref. 73.

9. The Reaction  $\gamma A \rightarrow V^0 A$  on Complex Nuclei

In the experiments to be discussed now, one uses the nucleus as a reabsorbing and refracting target of variable thickness for the vector mesons. One can relate the differential cross section  $\frac{d\sigma_{coh}}{dt}$  for the coherent reaction



to the spin- and isospin-independent part  $\frac{d\sigma_o}{dt} (\gamma N \rightarrow V^0 N)$  of the photoproduction differential cross section on a single nucleon at  $t = 0$ , using an impact parameter approach, and taking account of reabsorption of the  $V^0$ , hence  $\sigma_{VN}$  enters:<sup>78,79</sup>

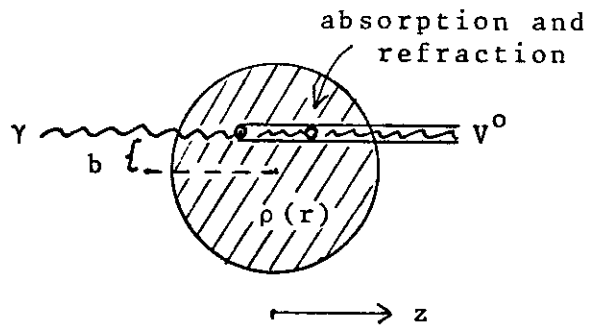
$$\frac{d\sigma_{coh}}{dt} = \frac{d\sigma_o}{dt} (\gamma N \rightarrow V^0 N) \Big|_{t=0} \left| \int_0^\infty 2\pi b db \int_{-\infty}^\infty dz J_0(b\sqrt{-t_\perp}) \rho(b, z) \exp(iz\sqrt{-t_\parallel}) \times \right.$$

$$\left. \times \exp \left[ -\frac{\sigma_{VN}}{2} (1 - i\alpha_{VN}) \int_z^\infty dz' \rho(b, z') \right] \right|^2$$

Here  $\sqrt{-t_\parallel}$  and  $\sqrt{-t_\perp}$  are the longitudinal and transverse four-momentum transfers,  $\rho(b, z)$  is the nuclear density distribution (normalized to A),  $\alpha_{VN}$  the ratio of real to imaginary part of the forward  $V^0 N$  elastic scattering amplitude, and  $\sigma_{VN}$  the total vector-meson nucleon cross section. The factor  $\exp(iz\sqrt{-t_\parallel})$  results from the lengthening of the wavelength of the emerging vector meson relative to the incident photon, caused by the photon-vector meson mass difference.

The nucleus remains in the ground state,

$$\sqrt{|t|_{MIN}} \approx \frac{m_V^2}{2E_\gamma} \ll \frac{1}{R_{nucleus}}$$

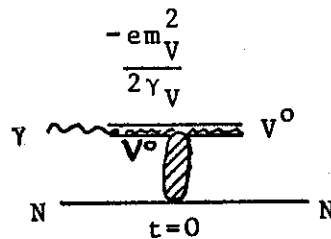


Corrections for nucleon-nucleon correlations (which can have a 10 % effect on the effective  $\sigma_{VN}$ ) have in some cases also been taken into account<sup>80</sup>.

As input for the analysis of the nuclear data with this model one uses the measured  $t$  and  $A$  dependence of the cross section for  $\gamma A \rightarrow V^0 A$  and the value of the ratio  $\alpha_{VN}$  of real to imaginary parts; further one has to adopt some model for the density distribution  $\rho(r)$ . One then obtains as output the values of  $\sigma_{VN}$  (where  $N$  stands for the average of the protons and neutrons in the nucleus) and of  $\left. \frac{d\sigma_0}{dt}(\gamma N \rightarrow V^0 N) \right|_{t=0}$ . In addition from the diffraction slope of  $\frac{d\sigma_{coh}}{dt}(\gamma A \rightarrow V^0 A)$  one can determine nuclear radii.

With these quantities one may test the vector dominance model and determine the photon-vector meson coupling constants, using the relation

$$\left. \frac{d\sigma_0}{dt}(\gamma N \rightarrow V^0 N) \right|_{t=0} = \frac{e^2}{4\gamma_V^2} \underbrace{\frac{\sigma_{VN}^2}{16\pi}}_{=(\text{Im}T_{VN})^2} (1 + \alpha_{VN}^2)$$



This simple relation holds only if contributions of intermediate vector meson states  $V^0, \neq V^0$  can be neglected.

A major uncertainty in the analysis of the photoproduction data on complex nuclei (but not on the deuteron, see section 8) is caused by the fact that the real parts of the  $V^0 N$  scattering amplitudes have a strong influence on the resulting nuclear photoproduction amplitudes<sup>81</sup>. Unfortunately direct measurement of the real parts is difficult and uncertainties are still large (see section 10). Therefore values estimated from vector dominance and total  $\gamma N$  cross sections using dispersion relations<sup>82</sup>, or from the real parts of  $\pi N$  and  $KN$  scattering with the additive quark model<sup>56,83</sup>, have also been used in the analysis of the data. It may be comforting that the procedure seems at least to be consistent, in that the imaginary parts (i.e. the total nucleon cross sections) which one then obtains, agree with the prediction from  $\pi N$  and  $KN$  scattering with the quark model (see below). The results on  $\sigma_{\rho^0 N}$  are also consistent with the values from double scattering in the deuteron (section 8), which are much less sensitive to the real parts.

As an example of the measurements that have been performed, Fig. 19 shows values of  $\frac{d\sigma}{d\Omega dM_{\pi\pi}}$  for  $\rho^0$  photoproduction on various nuclei, as obtained by the DESY-MIT-Group in a two-arm counter experiment at  $\langle E_\gamma \rangle = 6.2$  GeV.<sup>84</sup> About  $10^6$  events were collected in this experiment. The range of the square of the transverse four-momentum transfer is  $0.001 \text{ GeV}^2 < |t| < 0.01 \text{ GeV}^2$ . From these measured differential cross sections one has to subtract the "incoherent" background (with excitation or breakup of the nucleus, which is non-negligible on light nuclei)<sup>85</sup>. One also has, similar as with proton photoproduction data, to separate the  $\rho^0$  production from the non- $\rho^0$  background, using suitable models for the latter (e.g. phase space, or Drell process) to fit the  $M_{\pi^+\pi^-}$  distribution. The uncertainties on the final results of the experiment mainly stem from this background subtraction.

Measurements of  $\rho^0$  photoproduction have also been done by the Cornell<sup>59,86</sup>, Rochester<sup>87</sup> and SLAC<sup>88</sup> groups in the energy range from 5 to 16 GeV. The Cornell group used a two-arm spectrometer with spark chambers, while the Rochester and SLAC groups used large spark chamber systems. The angular acceptance in the SLAC experiment allowed to verify that the  $\rho^0$ 's are indeed transversally polarized. The results from these various experiments are consistent among each other. The value obtained of

$$\left. \frac{d\sigma}{dt}(\gamma N \rightarrow \rho^0 N) \right|_{t=0} \approx 118 \text{ } \mu\text{b GeV}^{-2}$$

is compatible with the  $\rho^0$  forward cross section on single protons (Section 6). The results on  $\sigma_{\rho N}$  and  $\gamma_\rho^2/4\pi$  from the various experiments are compiled in Fig. 20. Average values obtained are

$$\frac{\gamma_\rho^2}{4\pi} \sim 0.65, \quad \sigma_{\rho N} \approx 27 \text{ mb} \quad (\text{at } E_\gamma = 5 - 16 \text{ GeV}),$$

(photon mass shell)

in agreement with the Orsay value<sup>68</sup> of  $\gamma_\rho^2/4\pi = 0.64 \pm 0.06$  on the  $\rho$  mass shell. The value for  $\sigma_{\rho N}$  is in good agreement with



the additive quark model prediction

$$\sigma_{\rho^0 p} = \sigma_{\omega p} = \frac{1}{2}(\sigma_{\pi^+ p} + \sigma_{\pi^- p}) = \begin{cases} 28 \text{ mb} & \text{at } 5 \text{ GeV} \\ 25 \text{ mb} & \text{at } 14 \text{ GeV.} \end{cases}$$

The values for both  $\gamma_\rho^2/4\pi$  and for  $\sigma_{\rho^0 p}$  are also compatible with the results from the SLAC experiment on double-scattering in the deuteron<sup>70</sup>.

Results from  $\omega$  photoproduction on complex nuclei are shown in Table II. The Rochester group<sup>89</sup> has detected the  $\pi^+\pi^-\pi^0$  decay while the Bonn-Pisa group<sup>90</sup> measured the  $\pi^0\gamma$  decay of the  $\omega$ . Problems with large width, as for the  $\rho$ , are absent here but there is higher incoherent background, due to the pion exchange contribution to  $\omega$  production on nucleons. The values obtained for  $\left. \frac{d\sigma_o}{dt}(\gamma N \rightarrow \omega N) \right|_{t=0}$  agree, within the rather wide errors, with

Table II. Results from the Reaction  $\gamma A \rightarrow \omega A$

Group	$E_\gamma$ (GeV)	$\left. \frac{d\sigma_o}{dt}(\gamma N \rightarrow \omega N) \right _{t=0}$ [ $\mu\text{b GeV}^{-2}$ ]	$\sigma_{\omega N}$ (mb)	$\gamma_\omega^2/4\pi$
Rochester (Cornell) <sup>89</sup>	6.8	$11.4 \pm 1.9$	$25.3 \pm 7.8$	$7.6^{+1.8}_{-1.1}$
Bonn-Pisa (DESY) <sup>90</sup>	5.7	$15.1 \pm 3.1$	$30.0^{+7.0}_{-6.0}$	$5.8 \pm 1.3$
(Orsay $e^+e^- \rightarrow \omega$ ) <sup>68</sup>				$(4.8 \pm 0.5)$

the natural  $J^P$ -exchange contribution in the reaction  $\gamma p \rightarrow \omega p$  (see section 6). This is consistent with the  $A_2$  exchange contribution to  $\omega$  photoproduction on protons being rather small. The  $\sigma_{\omega N}$  values obtained are seen to be compatible with the quark model prediction of  $\sim 28$  mb.

Experiments on  $\phi$  photoproduction on complex nuclei<sup>6,37,65</sup> are quite difficult since the  $\phi$  is measured via its decay into  $K^+K^-$ , the angle between the kaon's momenta being very small, and the kaon's decay so rapidly that only a small fraction of them are detected and the decay products may cause background. The

results are summarized in Table III. The forward differential cross section  $\left. \frac{d\sigma_o}{dt}(\gamma N \rightarrow \phi N) \right|_{t=0}$  is consistent with the forward

Table III. Results from the Reaction  $\gamma A \rightarrow \phi A$

Group	$E_\gamma$ (GeV)	$\left. \frac{d\sigma_o}{dt}(\gamma N \rightarrow \phi N) \right _{t=0}$ ( $\mu\text{b GeV}^{-2}$ )	$\sigma_{\phi N}$ (mb)	$\gamma_\phi^2/4\pi$
Cornell <sup>65</sup>	6.4, 8.3	4.3	12	$5.8 \pm 2.4$
DESY-MIT <sup>6,37</sup>	5.2	$3.2 \pm 0.3$	$11.3 \pm 3$	$3.8 \pm 1.4$
(Orsay $e^+e^- \rightarrow \phi$ ) <sup>68</sup>				$(2.75 \pm 0.22)$

differential cross section for  $\phi$  production on protons (Section 6). A striking result is the smallness of the values for  $\sigma_{\phi N}$  obtained, compared with  $\sigma_{\rho^0 N}$ ,  $\sigma_{\omega N}$  and any other known total hadronic cross section. An explanation of this remarkable fact is given by the simple additive quark model<sup>56</sup>. The  $\phi$ , as a nearly pure  $(\lambda\bar{\lambda})$  state, interacts with the nucleon in this model only through strange - non strange quark-quark scattering, which is assumed to have a smaller cross section than the scattering between nonstrange quarks. The simple prediction from this model,

$$\sigma_{\phi p} = \sigma_{K^+p} + \sigma_{K^-n} - \sigma_{\pi^+p} = 13 \text{ mb} \quad \text{at } 5 \text{ GeV},$$

is in perfect agreement with the measured values of  $\sigma_{\phi N}$  given in Table III.

Summarizing the results on the photon-vector meson coupling constants  $\gamma_V^2/4\pi$ , their values (at  $k^2 = 0$ ) as obtained from  $V^0$  photoproduction on nuclei agree with the Orsay value<sup>68</sup> (at  $k^2 = m_V^2$ ) in the case of the  $\rho$ , and are perhaps somewhat larger than the Orsay values for  $\omega$  and  $\phi$ . The ratio

$$\frac{1}{\gamma_\rho^2} : \frac{1}{\gamma_\omega^2} : \frac{1}{\gamma_\phi^2} = 9 : (0.9 \pm 0.3) : (1.5 \pm 0.5) \quad \text{from } \gamma A \rightarrow V^0 A$$

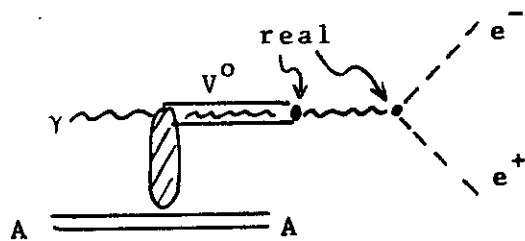
is still compatible with the expected ratio of  $9 : 0.65 : 1.33$ <sup>91</sup>.

Thus within the relatively big errors (caused to large extent by the uncertainty in the real parts), vector-dominance seems to do reasonably well in relating  $V^0$  photoproduction with  $V^0$  elastic scattering. This could be a hint that the failure of the vector dominance model in relating  $\gamma N$  scattering with the sum of the vector-meson photoproduction amplitudes (see section 7) is not primarily due to a  $k^2$  dependence of the coupling constants  $\gamma_V$ .

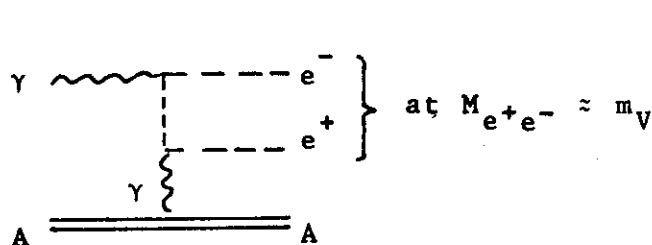
### 10. The Phase of the $\rho$ , $\omega$ and $\phi$ Forward Elastic Scattering Amplitudes

From the polarization and energy dependence of the reaction  $\gamma p \rightarrow \rho^0 p$  we were led to the conclusion that  $P$  is the dominant exchange. If this is correct then the ratio of the real to the imaginary part of the spin-independent forward amplitude of this reaction will be small at high energy. From the vector-dominance picture we then expect the corresponding ratio for elastic  $\rho^0 p$  scattering to be similarly small.

The phase of the vector meson photoproduction amplitude near the forward direction can be measured by observing its interference with the purely real Bethe-Heitler wide-angle lepton pair production amplitude which can be calculated in quantum-electrodynamics. In order to have identical final states one has to observe the  $e^+e^-$  or  $\mu^+\mu^-$  decays of the vector mesons:



(phase = phase of  $T_{\gamma A \rightarrow V^0 A}$   
 × phase of Breit-Wigner)



(real Bethe-Heitler amplitude)

at  $M_{e^+e^-} \approx m_V$

Since in the photoproduction amplitude the  $e^+e^-$  system couples to one photon, it has  $C = -1$ ; whereas in the Bethe-Heitler graph the coupling is to two photons and thus  $C = +1$ . Consequently the interference term in the cross section is asymmetric under the interchange of  $e^+$  and  $e^-$  (i.e. keeping the momenta fixed and interchanging the charges). One can therefore detect this interference term by varying e.g.  $p_{\perp,e^+} - p_{\perp,e^-} \hat{=} p_{e^+\theta} e^+ - p_{e^-\theta} e^-$  (where  $p_{\perp}$  is the transverse momentum), as shown in Fig. 21 from an experiment of the DESY-MIT group at 4.6 - 6.1 GeV on a Be target<sup>92</sup>. For "symmetric pairs"  $p_{\perp,e^+} = p_{\perp,e^-}$  and the interference term must vanish. One sees from Fig. 21 that the interference is large in the  $\rho^0$  region of  $e^+e^-$  masses, where the  $\rho$  Breit-Wigner phase is  $\approx \frac{\pi}{2}$ . This immediately shows that  $T_{\gamma A \rightarrow \rho^0 A}$  must be predominantly imaginary. The phase of the photoproduction amplitude on a single nucleon does not differ much from that of the nuclear amplitude, but detailed analysis has to take account of the phase change due to rescattering of the  $\rho^0$  in the nucleus.

The result of the DESY-MIT experiment<sup>92</sup> for the ratio of real to imaginary parts of the  $\rho^0$  photoproduction amplitude on single nucleons is

$$\alpha_{\rho N} = -0.2 \pm 0.1 \quad \text{at} \quad \langle E_{\gamma} \rangle \approx 5 \text{ GeV}$$

(see Fig. 21b). A similar experiment at NINA<sup>93</sup> on a C nucleus target gave

$$\alpha_{\rho N} = -0.28 \pm 0.12 \quad \text{at} \quad \langle E_{\gamma} \rangle = 4 \text{ GeV.}$$

The large error in these results is mainly due to the high sensitivity to the uncertainties in the value of the  $\rho^0$  mass. In a third experiment, measuring electroproduction of  $\rho^0 \rightarrow \mu^+ \mu^-$  from C at CEA, the presence of a real part of the  $\rho$  photoproduction amplitude was also indicated<sup>94</sup>. The results for  $\alpha_{\rho N}$  agree with the prediction  $\alpha_{\rho N} \hat{=} -0.2$  at  $E_{\gamma} = 4 - 6$  GeV of the simple additive quark model<sup>56,83</sup> via the relation to  $\pi N$  scattering amplitudes (as given in section 6). They are also compatible with the values of  $\alpha_{\gamma N}$  calculated from total photoproduction cross section data using the forward dispersion relation<sup>82</sup>.

The  $\phi$  photoproduction phase has recently also been observed by the DESY-MIT group with the result<sup>95</sup>

$$\alpha_{\phi N} = -0.48 \begin{matrix} +0.33 \\ -0.45 \end{matrix} \quad \text{at } \langle E_{\gamma} \rangle = 6.6 \text{ GeV.}$$

The additive quark model gives  $\alpha_{\phi N} = -0.3 \pm 0.45$  in the energy range of  $E_{\gamma} = 7 - 15 \text{ GeV}$ <sup>83</sup>.

The  $\omega$  nuclear photoproduction phase has been measured relative to the  $\rho^0$  production phase, by observing  $\rho/\omega$  interference in the  $e^+e^-$  mass spectrum of the reaction  $\gamma A \rightarrow e^+e^-A$ . (The Bethe-Heitler interference terms may in this case be cancelled out by observing "symmetric pairs", i.e. keeping the experimental acceptance symmetric under interchange of  $e^+$  and  $e^-$ .) Measured relative phases are

NINA:<sup>92,96</sup>  $(118_{-22}^{+13})$  deg (at  $E_{\gamma} = 4 \text{ GeV}$  on C nucleus)

DESY-MIT:<sup>97</sup>  $(41 \pm 20)$  deg (at  $E_{\gamma} = 5.1 \text{ GeV}$  on Be nucleus)

From these phase differences the effects of  $\rho/\omega$  mixing (which can amount to something like 20 deg) still have to be subtracted<sup>98</sup>. A detailed discussion of these results is given in the talk on electromagnetic decays of vector mesons by Prof. S. Ting.

### 11. Photoproduction of heavy (vector) mesons<sup>99</sup>

Of the searches for photoproduction of vector mesons<sup>100-105</sup> heavier than the  $\phi$ , the most intriguing result is still the one of Fig. 22. It shows, on a logarithmic scale, the  $\pi^+\pi^-$  mass distribution in the reaction

$$\gamma C \rightarrow \pi^+\pi^- + \text{anything}$$

at  $E_{\gamma} = 5.4 - 6.8 \text{ GeV}$  and  $|t_{\perp}| \leq 0.01 \text{ GeV}$ , measured by the DESY-MIT group<sup>103</sup>. The curve is the sum of the coherent and incoherent forward production cross sections according to a closure calculation by Trefil<sup>85</sup>, multiplied with a Breit-Wigner function and a

factor  $M_{\pi\pi}^{-4,54}$  plus a non- $\rho$  background term, polynomial in  $\pi^+\pi^-$  mass. There appears a shoulder in the 1300 - 1800 MeV region, for which no satisfactory explanation seems to have been found. A similar effect has been observed by the SLAC group at 16 GeV on a Be target<sup>102</sup>. It cannot be a reflection from e.g.  $\Delta(1236)$  production since only symmetrically decaying dipions were detected in the experiment, and these do not overlap with the  $\Delta(1236)$  bands in the Dalitz plot (compare Fig. 2). There could of course be some background from reactions with additional undetected pions. The experiment has been repeated on a hydrogen target, with a similar result<sup>106</sup>.

Figure 23 shows the  $\pi^+\pi^-$  mass distribution from a compilation of various bubble and streamer chamber experiments (all of which had essentially complete decay angular acceptance for the  $\pi^+\pi^-$  system) at energies above 4 GeV<sup>17,25,61,62,66</sup>. The broad shoulder at the high-mass side of the  $\rho^0$  may here be partly due to reflection from  $\Delta^{++}(1236)$  decays.

Since decay into charged lepton pairs is allowed for any vector meson coupled to the photon, searches in the  $\mu^+\mu^-$  mass spectrum have particular significance<sup>104,105</sup>. In the mass region surveyed,  $m_\phi < M_{\mu^+\mu^-} < 2100$  MeV, no vector meson was found within a cross section level of a few percent of  $\sigma_\rho$ .

An experiment in which the search was not restricted to vector mesons, or mesons decaying into  $\pi^+\pi^-$ , was done at SLAC<sup>45</sup>. Here the reaction

$$\gamma p \rightarrow p + \text{missing mass}$$

was measured in the energy range of 16 - 17.8 GeV, detecting only the proton and using bremsstrahlung end-point subtraction. Nothing was found in the 1 - 2 GeV range of masses. The upper limit (at a 90 % confidence level) of the cross section for production of any meson with  $1.3 \text{ GeV} < M < 2 \text{ GeV}$  and  $\Gamma \leq 200 \text{ MeV}$  from this experiment is 5 % of the  $\rho^0$  production cross section. Note however that the  $\phi$  cross section, at 16 GeV, is already below this limit.

The SLAC group did observe however a bump in the missing-mass spectrum at about 1240 MeV, at a photon energy of  $E_\gamma \approx 14$  GeV<sup>45</sup>. This observation was confirmed in the bubble chamber experiment of the SBT collaboration<sup>29</sup> and in the DESY streamer chamber experiment<sup>61</sup>, where the enhancement was found to occur in the pionic system of the reaction

$$\gamma p \rightarrow p \pi^+ \pi^- + n \pi^0 \quad (n \geq 2)$$

at  $E_\gamma$  between 3 and 6 GeV. Mass and width (1250 MeV and 100 MeV, respectively) of this effect suggest that it may be due to the  $B^0(1235)$ , probably an axial vector meson which decays into  $\omega + \pi^0$ . Indeed a selection of  $\pi^+ \pi^-$  states in the kinematic region where the  $\omega$  decay matrix element is largest, was found to enhance the effect. Since this effect, supposedly B meson production, has similar cross sections from 3 to 14 GeV, it is interesting to speculate that it may be a diffractive process ( $\mathbb{P}$  exchange).

The searches discussed so far did not extend much beyond 2 GeV in mass. The SLAC streamer chamber group has searched for vector mesons of mass up to 3.5 GeV, decaying into four pions, in the reaction

$$\gamma p \rightarrow \pi^+ \pi^- \pi^+ \pi^- p$$

at  $E_\gamma = 6 - 18$  GeV<sup>107</sup>. They have found an enhancement with mass  $M_{4\pi} \approx 1600$  MeV and a width of several 100 MeV. Its interpretation is not yet clear.

There are several reasons to expect vector mesons heavier than the  $\phi$  to exist. In the quark model the  ${}^3D_1$  rotational level is a  $J^{PC} = 1^{--}$  nonet, with masses expected to be somewhere in the 1500 - 2000 MeV region. The Veneziano model predicts a  $\rho'$  at 1250 MeV (degenerate with the  $f$ ) and a  $\rho''$  at 1650 MeV (degenerate with the  $g$ )<sup>108</sup>. Coherent diffractive photoproduction was expected to be an effective "filter" for vector meson states. It has however been argued recently on the basis of a multiperipheral production mechanism and duality, that even with rather large couplings of these heavy mesons to the photon the resulting

photoproduction cross sections will still be small enough so that the  $\rho'$  could have remained undetected until now<sup>109</sup>. For the quantity (production cross section)  $\times$  (branching fraction into  $\pi^+\pi^-$ ), empirical upper limits at  $E_\gamma = 9$  GeV of  $0.5 \mu\text{b}$  for  $\rho'$  and  $0.2 \mu\text{b}$  for  $\rho''$  have been established, provided the width of these states does not exceed 200 MeV<sup>19\*</sup>.

It may be interesting to briefly list the experimental evidence on photoproduction of other mesons of the natural  $J^P$  series.

- (i)  $J^{PC} = 0^{++}$  ( $\gamma p \rightarrow \epsilon p$ ): No indication has been seen. The main argument for small cross section is the zero forward/backward asymmetry of the  $\pi^+\pi^-$  decays in the  $\rho^0$  mass region (in contrast e.g. to the reaction  $\pi^-p \rightarrow \pi^+\pi^-n$ ).<sup>17,25</sup>
- (ii)  $J^{PC} = 2^{++}$ : Of the reaction  $\gamma p \rightarrow f p$  at most slight indications have been seen. Only a limit of  $\sigma \leq 0.4 \mu\text{b}$  in the energy region of 2.5 - 5 GeV can be stated<sup>17,25</sup>. The reaction  $\gamma p \rightarrow A_2^+ n$  has been reported and seems to occur with a cross section of  $\sim 1 \mu\text{b}$  in the 4 - 5 GeV energy region<sup>29,62,111</sup>. No firm evidence for the reaction  $\gamma p \rightarrow A_2^0 p$  has been found (in contrast to charged  $A_2$  photoproduction, pion exchange does not contribute here), so only a limit of  $\leq 1 \mu\text{b}$  for  $E_\gamma = 2.5 - 6$  GeV (at the 90 % confidence level) can be quoted<sup>25,29,62</sup>.
- (iii)  $J^{PC} = 3^{--}$  ( $\gamma p \rightarrow g p$ ): This reaction has not yet been observed.

#### Acknowledgement

I would like to thank U. Becker, E. Lohrmann, H. Meyer, W.J. Podolsky, A.H. Rosenfeld and G. Wolf for valuable discussions on the subjects covered in this talk.

---

\* In the reaction  $\bar{p}p \rightarrow K_S^0 K_L^0$  evidence suggestive of a vector meson with  $M = 1968$  MeV and  $\Gamma = 35$  MeV has recently been reported<sup>110</sup>.



References

1. J.J. Sakurai, Ann. Phys. 11, 1 (1960);  
M. Gell-Mann and F. Zachariasen, Phys. Rev. 124, 953 (1961);  
M. Gell-Mann, Phys. Rev. 125, 1067 (1962);  
N.M. Kroll, T.D. Lee, and B. Zumino, Phys. Rev. 157, 1376  
(1967)
2. J.J. Sakurai, Proceedings of the 4th International Symposium  
on Electron and Photon Interactions at High Energies,  
Liverpool 1969, p.91;  
D. Schildknecht, Z. Physik 229, 278 (1969).  
See also Refs. 4, 5, and 8.
3. SLAC-Berkeley-Tufts Collaboration, Phys. Rev. Letters 24,  
960, 1467(E) (1970)
4. K. Lübelmeyer, Meson Photoproduction, Rapporteur Talk at  
the XVth International Conference on High Energy Physics,  
Kiev (1970); Bonn University preprint PIB 1-126 (1971)
5. G. Wolf, Photoproduction of Vector Mesons, Invited talk  
presented at the Symposium on Meson Photo- and Electro-  
production at low and intermediate Energies, University of  
Bonn (1970), DESY-70/64 (1970) and Springer Tracts in Modern  
Physics, Vol. 59 (1971), to be published
6. R. Marshall, Photoproduction of Vector Mesons, Talk presented  
at the Daresbury Study Weekend on Vector Meson Production  
and Omega-Rho Interference (1970), DESY-70/32 (1970)
7. U. Maor, Nucl. Phys. B 24, 1 (1970)
8. D.W.G.S. Leith, in Hadronic Interactions of Electrons and  
Photons (Ed. J. Cumming and H. Osborn), 1971, p.195
9. P.L. Braccini, Vector Meson Photoproduction, in Proceedings  
of the V<sup>e</sup> Rencontre de Moriond sur les Interactions Electro-  
magnétiques, p. II.94 (1970)
10. A. Silverman, in Proceedings of the 4th International  
Symposium on Electron and Photon Interactions at High Energies,  
Liverpool 1969, p.71

11. E. Lohrmann, in Proceedings of the Lund International Conference on Elementary Particles, Lund 1969, p.13
12. H. Überall, Phys. Rev. 103, 1055 (1956); 107, 223 (1957);  
G. Barbiellini et al., Phys. Rev. Letters 8, 112 (1962)
13. G. Diambri-Palazzi, Rev. Mod. Phys. 40, 611 (1968);  
U. Timm, Fortschr. Physik 17, 765 (1969)
14. R.H. Milburn, Phys. Rev. Letters 10, 75 (1963)
15. F.R. Arutyunian and V.A. Tumanian, Phys. Letters 4,  
176 (1963)
16. C.K. Sinclair et al., IEEE Trans. on Nucl. Sci. 16,  
1065 (1969)
17. SLAC-Berkeley-Tufts Collaboration, Phys. Rev. Letters  
24, 955 (1970); 24, 960, 1467(E) (1970);  
SLAC-PUB-941 (1971), to be published;  
K.C. Moffeit, UCRL-19890 (1970), unpublished
18. SLAC-Berkeley-Tufts Collaboration, Phys. Rev. Letters  
24, 1364 (1970); 26, 155(E) (1971);  
W.J. Podolsky, UCRL-20128 (1971), unpublished
19. SLAC-Berkeley-Tufts Collaboration, Bull. Am. Phys. Soc.  
16, 549 (1971), and private communication
20. G. McClellan et al., Phys. Rev. Letters 26, 1597 (1971)
21. C. Berger et al., Phys. Rev. Letters 25, 1366 (1970)
22. M. Jacob and G.C. Wick, Ann. Phys. 7, 404 (1959)
23. K. Schilling, P. Seyboth and G. Wolf, Nucl. Phys. B 15,  
397 (1970)
24. C. Zemach, Phys. Rev. 140, B 97 (1965)
25. Aachen-Berlin-Bonn-Hamburg-Heidelberg-Munich Collaboration,  
Phys. Rev. 175, 1669 (1968)
26. R.K. Adair, Phys. Rev. 100, 1540 (1955); Rev.Mod.Phys. 37,  
473 (1965);  
Y. Eisenberg et al., Phys. Letters 22, 223 (1966);  
G. Kramer, DESY-67/32 (1967), unpublished

27. K. Gottfried and J.D. Jackson, Nuovo Cimento 33, 309 (1964);  
J.D. Jackson, Nuovo Cimento 34, 1644 (1964)
28. Aachen-Berlin-Bonn-CERN-Cracow-Heidelberg-London-Vienna  
Collaboration, Phys. Letters 34B, 160 (1971);  
G. Ascoli et al., Phys. Rev. Letters 26, 929 (1971);  
F. Grard et al., Lettere Nuovo Cimento 2, 305 (1971)
29. W.J. Podolsky, UCRL-20128 (1971), unpublished
30. L. Criegee et al., Phys. Rev. Letters 25, 1306 (1970)
31. G. Diambri-Palazzi et al., Phys. Rev. Letters 25, 478 (1970)
32. G. Wolf, private communication; see also ref. 5
33. M. Houtebeyrie et al., Phys. Letters 36B, 98 (1971)
34. S. Rai Choudhury and R. Rajaraman, University of Delhi  
preprint (1971)
35. J. Benecke and H.P. Dürr, Nuovo Cimento 56A, 269 (1968)
36. G. Wolf, Phys. Rev. 182, 1538 (1969)
37. S.C.C. Ting, in Proceedings of the 14th International  
Conference on High Energy Physics, Vienna 1968, p.43.  
(See also U. Becker et al., Phys. Rev. Letters 21, 1504 (1968))
38. C. Berger et al., Cornell University preprint  
CLNS-168 (1971), submitted to Phys. Rev.
39. G. Cosme, Measurement of the radiative decay modes of the  
 $\phi$  meson with the Orsay storage ring, presented at the  
International Conference on Meson Resonances and related  
electromagnetic Phenomena, Bologna, April 1971. (The partial  
widths quoted were obtained by multiplying the Orsay  
branching fractions by  $\Gamma_{\phi} = 4$  MeV.)
40. Aachen-Berlin-Bonn-Hamburg-Heidelberg-Munich Collaboration,  
Phys. Letters 27B, 54 (1968); Phys. Rev. 188, 2060 (1969)
41. P.G.O. Freund, Nuovo Cimento 48A, 541 (1967)
42. V. Barger and D. Cline, Phys. Rev. Letters 24, 1313 (1970)

43. G. Wolf, Nucl. Phys. B26, 317 (1971)
44. This comment does not apply to the SLAC experiment of Bulos et al., discussed in detail by D.W.G.S. Leith in ref. 8
45. R. Anderson et al., Phys. Rev. D1, 27 (1970)
46. S.D. Drell, Phys. Rev. Letters 5, 278 (1960); Rev. Mod. Phys. 33, 458 (1961)
47. P. Söding, Phys. Letters 19, 702 (1966)
48. A. Krass, Phys. Rev. 159, 1496 (1967)
49. T. Bauer, Phys. Rev. Letters 25, 485, 704(E) (1970)
50. J. Pumplin, Phys. Rev. D2, 1859 (1970)
51. D.R. Yennie, in Hadronic Interactions of Electrons and Photons (Ed. J. Cumming and H. Osborn), 1971, p.321
52. G. Kramer, Recent Theoretical Work in Photoproduction of vector mesons, Daresbury Meeting on  $\omega\rho$  Mixing, 1970, DESY T-70/4 (1970);  
F. Gutbrod, private communication
53. H. Satz and K. Schilling, Nuovo Cimento 67A, 511 (1970);  
P. Dewey and B. Humpert, Cavendish Laboratory preprint HEP 71-2 (1971)
54. M. Ross and L. Stodolsky, Phys. Rev. 149, 1172 (1966);  
G. Kramer and J.L. Uretsky, Phys. Rev. 181, 1918 (1969);  
P.D. Mannheim and U. Maor, Phys. Rev. D2, 2105 (1970);  
G. Kramer and H.R. Quinn, Nucl. Phys. B27, 77 (1971);  
G. Kramer, DESY preprint 71/40 (1971)
55. Particle Data Group, Rev. Mod. Phys. 43, S 1
56. H.J. Lipkin, Phys. Rev. Letters 16, 1015 (1966);  
H. Joos, in Hadronic Interactions of Electrons and Photons (Ed. J. Cumming and H. Osborn), 1971, p.47;  
K. Kajantie and J.S. Trefil, Phys. Letters 24B, 106 (1967)

57. K.J. Foley et al., Phys. Rev. Letters 11, 425 (1963);  
11, 503 (1963); 15, 45 (1965)
58. H. Alvensleben et al., Phys. Rev. Letters 23, 1058 (1969);  
Nucl. Phys. B18, 333 (1970)
59. G. McClellan et al., Cornell University preprint CLNS-154  
(1971), submitted to Phys. Rev. See also Refs. 38 and 75
60. F. Bulos et al., discussed by D.W.G.S. Leith in-ref. 8
61. Aachen-Hamburg-Heidelberg-Munich Streamer Chamber Collaboration,  
to be published;  
E. Rabe, internal report DESY F1-71/2 (1971)
62. Y. Eisenberg et al., Phys. Rev. Letters 22, 669 (1969);  
J. Ballam et al., Phys. Letters 30B, 421 (1969);  
J. Ballam et al., SLAC-Weizmann-Tel Aviv preprint (1971)
63. Y. Eisenberg et al., Phys. Letters 34B, 439 (1971)
64. K. Schilling and F. Storim, Nucl. Phys. B7, 559 (1968).  
The calculation was done using a sharp cutoff at impact  
parameters  $R \leq 0.8 F$ , and with  $\Gamma_{\omega\pi\gamma} = 1.2 \text{ MeV}$ .
65. G. McClellan et al., Phys. Rev. Letters 26, 1593 (1971);  
see also Ref. 38
66. M. Davier et al., Phys. Rev. D1, 790 (1970)
67. L. Stodolsky, Phys. Rev. Letters 18, 135 (1967)
68. J.C. Bizot, Phys. Letters 32B, 416 (1970). For  $\gamma_{\rho}^2/4\pi$  and  
 $\gamma_{\omega}^2/4\pi$  we take here the new values reported by the Orsay  
group at the Amsterdam International Conference on Elementary  
Particles (1971).
69. D.O. Caldwell et al., Phys. Rev. Letters 25, 609 (1970)
70. R.L. Anderson et al., preprint SLAC-PUB-916 (1971)
71. V. Franco and R.J. Glauber, Phys. Rev. 142, 1195 (1966);  
R.J. Glauber, Lectures in Theoretical Physics, Boulder (1958),  
Vol. I, p.315

72. Aachen-Bonn-Hamburg-Heidelberg-Munich Collaboration, Nucl. Phys. B23, 45 (1970); and private communication
73. Y. Eisenberg et al., Weizmann Institute preprint WIS 71/9 Ph (1971)
74. Aachen-Bonn-Hamburg-Heidelberg-Munich Collaboration, Nucl. Phys. B21, 93 (1970); and private communication
75. G. McClellan et al., Phys. Rev. Letters 22, 374 (1969)
76. H.-J. Behrend et al., Phys. Rev. Letters 26, 151 (1971)
77. H. Meyer et al., Phys. Letters 33B, 189 (1970)
78. K.S. Kölbig and B. Margolis, Nucl. Phys. B6, 85 (1968); S.D. Drell and J.S. Trefil, Phys. Rev. Letters 16, 552, 832(E) (1966)
79. Excellent and detailed discussions of the experimental and theoretical problems have been presented by D.W.G.S. Leith (ref.8) and D.R. Yennie (ref.51) at the Scottish Universities Summer School in Physics, 1970
80. G. v. Bochmann, B. Margolis and L.C. Tang, Phys. Letters 30B, 254 (1969)
81. J. Swartz and R. Talman, Phys. Rev. Letters 23, 1078 (1969). See also ref. 10.
82. M. Damashek and F. Gilman, Phys. Rev. D1, 1319 (1970); H. Meyer et al., Desy report DESY 70/17 (1970)
83. S.A. Jackson and R.E. Mikkens, Lettere Nuovo Cimento 3,1 (1970); M. Krammer, Acta Physica Austriaca 32, 395 (1970); T.J. Weare, Lettere Nuovo Cimento 4, 251 (1970); K. Okada, Prog. Theo. Phys. 43,1574 (1970)
84. H. Alvensleben et al., Nucl. Phys. B18, 333 (1970); Phys. Rev. Letters 24, 786 (1970)
85. J.T. Trefil, Nucl. Phys. B11, 330 (1969); Phys. Rev. 180, 1379 (1969); K.S. Kölbig and B. Margolis, Nucl. Phys. B6, 85 (1968)

86. G. McClellan, Phys. Rev. Letters 22, 377 (1969)
87. H.-J. Behrend et al., Phys. Rev. Letters 24, 336 (1970)
88. F. Bulos et al., Phys. Rev. Letters 22, 490 (1969);  
see also ref. 8
89. H.-J. Behrend, Phys. Rev. Letters 24, 1246 (1970);  
Phys. Rev. Letters 27, 65 (1970)
90. P.L. Braccini et al., Nucl. Phys. B24, 173 (1970)
91. R.J. Oakes and J.J. Sakurai, Phys. Rev. Letters 19,  
1266 (1967)
92. H. Alvensleben et al., Phys. Rev. Letters 25, 1377 (1970)
93. P.J. Biggs et al., Daresbury preprint DNPL/P 70 (1971);  
E. Gabathuler, in Experimental Meson Spectroscopy  
(Ed. C. Baltay and A.H. Rosenfeld), 1970, p.645
94. D.R. Earles et al., Phys. Rev. Letters 25, 129 (1970)
95. H. Alvensleben et al., Phys. Rev. Letters 27, 444 (1971)
96. P.J. Biggs et al., Phys. Rev. Letters 24, 1197 (1970)
97. H. Alvensleben et al., Phys. Rev. Letters 25, 1373 (1970)
98. H.R. Quinn and T.F. Walsh, Nucl. Phys. B22, 637 (1970)
99. This has been reviewed recently by M. Davier, in Proceedings  
of the V<sup>e</sup> Rencontre de Moriond sur les Interactions Electro-  
magnétiques, p.II.45 (1970)
100. G. McClellan et al., Phys. Rev. Letters 23, 718 (1969)
101. N. Hicks et al., Phys. Letters 29B, 602 (1969)
102. F. Bulos et al., Phys. Rev. Letters 26, 149 (1971)
103. H. Alvensleben et al., Phys. Rev. Letters 26, 273 (1971)
104. S. Hayes et al., Phys. Rev. Letters 24, 1369 (1970)
105. D. Earles et al., Phys. Rev. Letters 25, 1312, (1738(E)) (1970)
106. S.C.C. Ting, private communication

107. M. Davier et al., SLAC-PUB-666 (1969); and private communication
108. G. Veneziano, Nuovo Cimento 57A, 190 (1968);  
J.A. Shapiro, Phys. Rev. 179, 1345 (1969);  
V. Barger and D. Cline, Phys. Rev. 182, 1849 (1969)
109. P.H. Frampton, K. Schilling and C. Schmid, preprint TH.1347-CERN (1971)
110. A. Benvenuti et al., Phys. Rev. Letters 27, 283 (1971)
111. Y. Eisenberg et al., Phys. Rev. Letters 23, 1322 (1969)



Figure Captions

- Fig. 1. Comparison of photon beam spectra. On the left, the coherent bremsstrahlung intensity (= number of photons  $\times$  photon energy) (full curve) and the calculated polarization (dashed curve) from a recent Cornell experiment are shown<sup>20</sup>. The right hand figure shows the measured  $e^+e^-$ -pair energy spectra (white histogram), and the energy spectra of fitted  $\gamma p \rightarrow \pi^+\pi^-p$  events (black histogram), produced by the laser backscattered beam at SLAC<sup>17</sup>.
- Fig. 2. Dalitz plot, and part of Chew-Low plot, for the reaction  $\gamma p \rightarrow \pi^+\pi^-p$  at  $E_\gamma = 9.3$  GeV.<sup>19</sup>
- Fig. 3. Distribution of the dipion angles  $\vartheta_H, \psi_H$  (in the helicity frame) in the reaction  $\gamma p \rightarrow \pi^+\pi^-p$  at  $E_\gamma = 9.3$  GeV, with cuts  $0.6$  GeV  $< M_{\pi^+\pi^-} < 0.85$  GeV and  $0.02$  GeV<sup>2</sup>  $< |t| < 0.4$  GeV<sup>2</sup> in the  $\rho^0$  region<sup>19</sup>. The curves are the angular distributions expected for s-channel helicity-conserving  $\rho^0$  production.
- Fig. 4. Angle  $\beta$  for rotation from the helicity frame into the "minimum flip system" (see text) as a function of  $|t|$ , for the reaction  $\gamma p \rightarrow \rho^0 p$  at  $E_\gamma = 9.3$  GeV and  $4.7$  GeV<sup>17,19</sup>. The curves marked H, A and GJ show where the data points should be if the minimum flip system were the helicity, Adair and Gottfried-Jackson frame, respectively.
- Fig. 5. Asymmetry ratio  $\Sigma$  in the reaction  $\gamma p \rightarrow \rho^0 p$  as a function of the photon energy  $E_\gamma$ .
- Fig. 6. Parity asymmetry  $P_\sigma$  in the reaction  $\gamma p \rightarrow \rho^0 p$  at  $E_\gamma = 9.3$  GeV as a function of  $t$ <sup>19</sup>.
- Fig. 7. The density matrix elements  $\rho_{00}^{(0)}$  and  $\rho_{1,-1}^{(1)}$  and the parity asymmetry  $P_\sigma$  in the reaction  $\gamma p \rightarrow \pi^+\pi^-p$  at  $2.8$  and  $4.7$  GeV for  $|t| < 0.4$  GeV<sup>2</sup>, as a function of  $M_{\pi^+\pi^-}$ <sup>17</sup>.

- Fig. 8. Helicity system decay angular distributions, and parity asymmetry  $P_{\sigma}$ , for  $\omega$  events ( $0.74 \text{ GeV} < M_{\pi^+\pi^-\pi^0} < 0.84 \text{ GeV}$ , without background subtraction) from the reaction  $\gamma p \rightarrow \pi^+\pi^-\pi^0 p$  at 2.8, 4.7 and 9.3 GeV<sup>17,19</sup>. The curves give the decay distributions resulting from the fitted helicity density matrix.
- Fig. 9. Total cross sections for the reaction  $\gamma p \rightarrow \omega p$  as a function of photon energy<sup>19</sup>. The points labeled "This Experiment", "DESY-HBC" and "SLAC Annihilation Beam" are from Ref. 19, Ref. 25 and Ref. 63, respectively. Also shown are the natural and unnatural exchange parts,  $\sigma^N$  and  $\sigma^U$ , found from the polarized beam experiments<sup>18,19</sup>. The curves show the pion exchange (full) and diffractive (dashed) parts<sup>19</sup>.
- Fig. 10. Differential cross section for the reaction  $\gamma p \rightarrow \rho^0 p$  for photon energies between 6.5 and 17.8 GeV, from Ref. 45. The curves are from a fit with the vector dominance and quark model relation (see text), with one adjustable parameter  $\gamma_{\rho}^2/4\pi$ .
- Fig. 11. Compilation of recent data on  $d\sigma/dt|_{t=0}$  for the reaction  $\gamma p \rightarrow \rho^0 p$ , as a function of photon energy.
- Fig. 12. Typical appearance of  $\rho^0$ ,  $\omega$  and  $\phi$  peaks (in the mass spectra of  $M_{\pi^+\pi^-}$ ,  $M_{\pi^+\pi^-\pi^0}$  and  $M_{K^+K^-}$ , respectively) in high-energy photoproduction. The data are from Refs. 18, 25 and 65.
- Fig. 13. Differential cross section for the reaction  $\gamma p \rightarrow \omega p$  in various photon energy intervals from 2 to 8.2 GeV.<sup>63</sup> The curves are from a fitted model, assuming diffraction and pion exchange (see text).
- Fig. 14. Differential cross section for the reaction  $\gamma p \rightarrow \phi p$  for photon energies between 2.5 and 12 GeV (from Ref. 65). The points labeled "CORNELL" are from Ref. 65, "DESY-MIT" from Ref. 37, "DESY-HBC" from Ref. 25, and "SLAC" from Ref. 45. The straight line represents a fit<sup>65</sup> to the Cornell data at 8.3 and 8.8 GeV.

- Fig. 15. Total cross section of the reaction  $\gamma p \rightarrow \phi p$  as a function of photon energy.
- Fig. 16. Differential cross sections for coherent  $\rho^0$  photo-production from deuterons (Ref. 70; figure taken from Ref. 4). The curves are obtained from fits, using Glauber theory, to the double-scattering region (see text).
- Fig. 17. Differential cross sections for coherent  $\rho^0$  photo-production from deuterons at small  $|t|$ .<sup>72</sup> The curves are predictions, calculated from Glauber theory under the assumption that  $\rho^0$  production on single nucleons is pure isoscalar exchange.
- Fig. 18. Total cross section for the reaction  $\gamma n \rightarrow \rho^- p$ , with the restriction  $|t| < 1.1 \text{ GeV}^2$ , as a function of photon energy<sup>74</sup>. No corrections for d effects are included. The solid curve shows the pion exchange prediction with  $\Gamma_{\rho\pi\gamma} = 0.13 \text{ MeV}$ . The dashed curve shows the qualitative behavior of  $\sigma(\gamma p \rightarrow \rho^0 p)$ .
- Fig. 19. Differential cross sections  $Z = d\sigma/d\Omega dM_{\pi\pi}$  ( $\mu\text{b/ster/MeV/nucleon}$ ) as a function of  $M_{\pi\pi}$  (MeV) and  $t$  (units  $-0.001 \text{ GeV}^2$ ), for the reaction  $\gamma A \rightarrow \pi^+ \pi^- \dots$  at  $E_\gamma = 6.2 \text{ GeV}$  and with various different  $A$ .<sup>84</sup> The curves are fits with a superposition of coherent and incoherent  $\rho^0$  production, and non- $\rho$  background.
- Fig. 20. Values of  $\gamma_\rho^2/4\pi$  and  $\sigma_{\rho N}$  as obtained from recent  $\rho^0$  photoproduction experiments on complex nuclei (Figure adapted from Ref. 4). Included are the results of the SLAC experiment on  $\rho^0$  scattering in the deuteron<sup>70</sup>, and the  $\rho$  mass-shell measurement of  $\gamma_\rho^2/4\pi$  from Orsay<sup>68</sup>.

Fig. 21. Reaction  $\gamma\text{Be} \rightarrow e^+e^-\text{Be}$  at 4 - 6 GeV <sup>92</sup>.  
(a) Measured difference  $N_+ - N_-$  of event numbers in the two arms of the spectrometer, as a function of the asymmetry  $\delta = p_{e^+} \theta_{e^+} - p_{e^-} \theta_{e^-}$ , in various regions of the  $\pi^+\pi^-$  mass. The curves are from fits with  $\alpha_{\rho N} = -0.2 \pm 0.1$ .  
(b) Fitted values of the deviation  $\varphi$  of the nuclear  $(\pi^+\pi^-)$ -photoproduction amplitude from  $\frac{\pi}{2}$  (left part), and of the ratio  $\beta = -\alpha_{\rho N} = -$  (real/imaginary) parts of the photoproduction amplitude on single nucleons (right part), as a function of the  $\pi^+\pi^-$  mass.

Fig. 22. Dipion mass spectrum of the reaction  $\gamma\text{C} \rightarrow \pi^+\pi^- + \dots$  at 5.4 - 6.8 GeV and  $|t_\perp| \leq 0.01 \text{ GeV}^2$  (Ref. 103). The cross sections are averaged over the spectrometer aperture. The errors are statistical only. The curve is approximated from a fit with a superposition of coherent and incoherent  $\rho$  production plus non- $\rho$  polynomial background, fitted in the  $\rho$  mass region (600 - 900 MeV) and extrapolated towards higher dipion masses.

Fig. 23. Dipion mass spectrum of the reaction  $\gamma p \rightarrow \pi^+\pi^- p$ , from a compilation of various bubble and streamer chamber experiments at energies above 3 GeV (Refs. 17, 25, 61, 62, 66). (In considering the significance of structures in distributions compiled from different experiments, one should keep in mind that the phase space distributions of the various experiments differ, due to different beam momenta.)

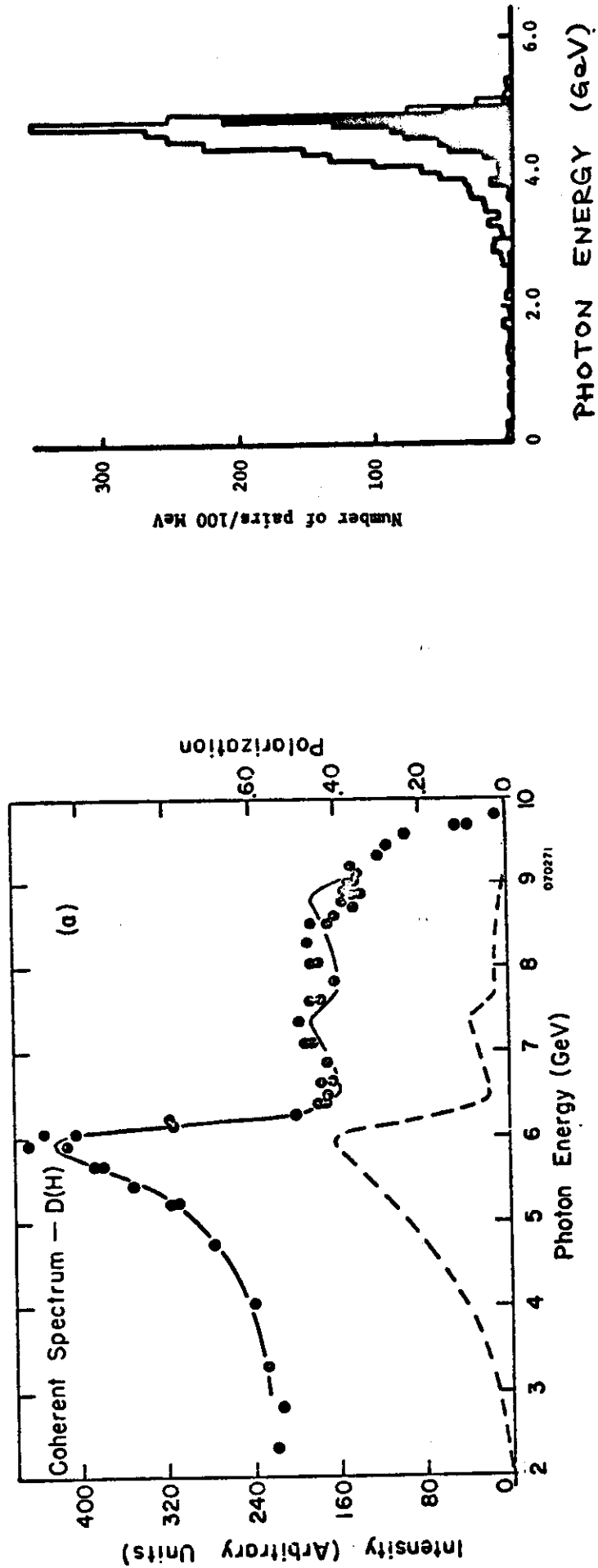


Fig. 1

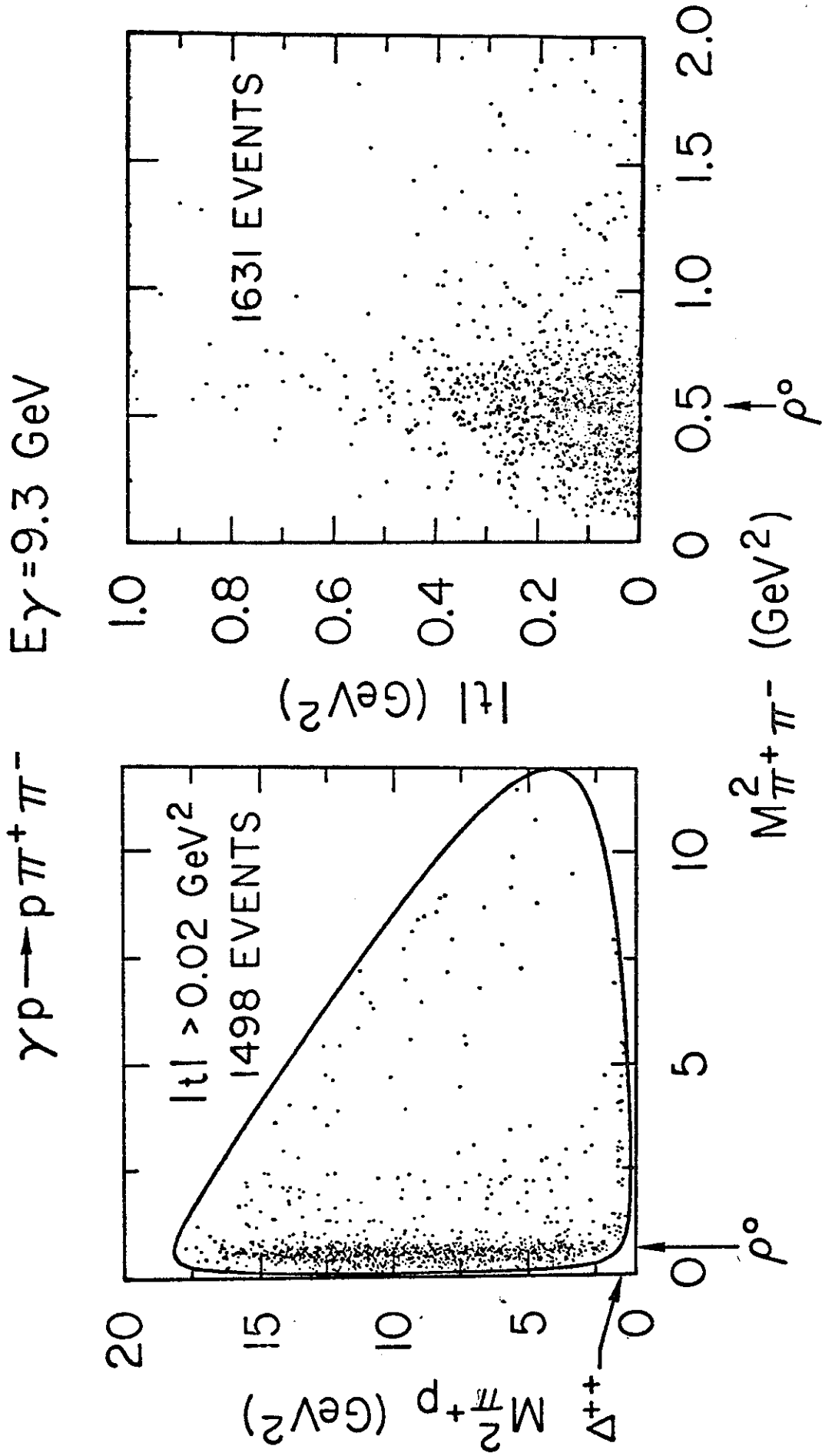
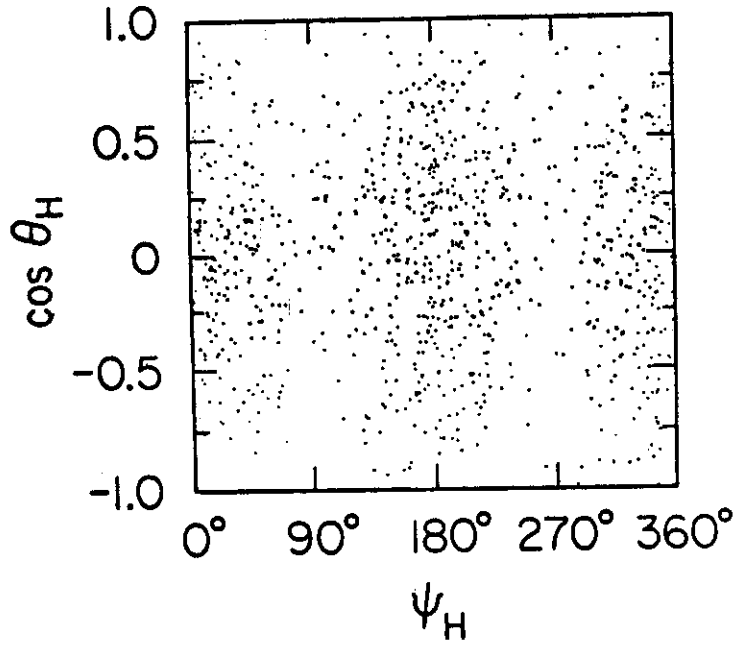
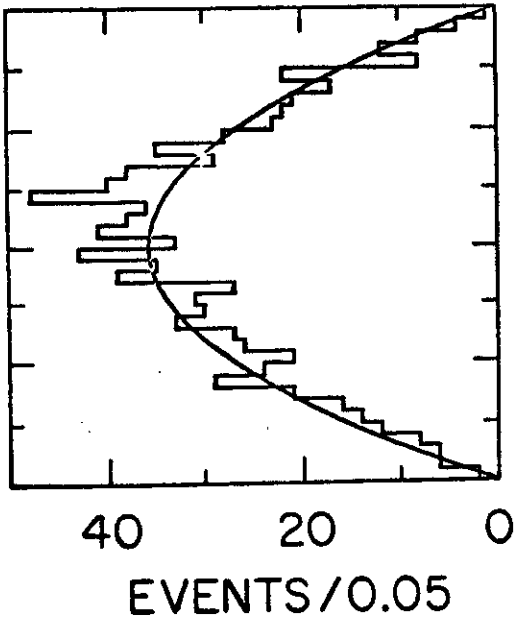


Fig. 2



$\gamma p \rightarrow p \pi^+ \pi^-$

$E_\gamma = 9.3 \text{ GeV}$

$0.6 < M_{\pi^+ \pi^-} < 0.85 \text{ GeV}$

$0.02 < |t| < 0.4 \text{ GeV}^2$

954 EVENTS

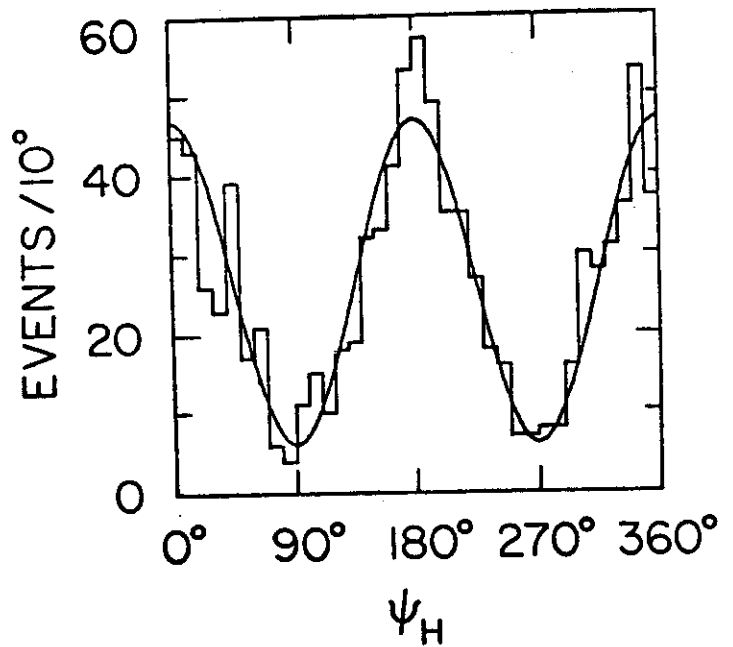


Fig. 3

$\gamma p \rightarrow p \rho^0$  ROTATION INTO MINIMUM FLIP SYSTEM

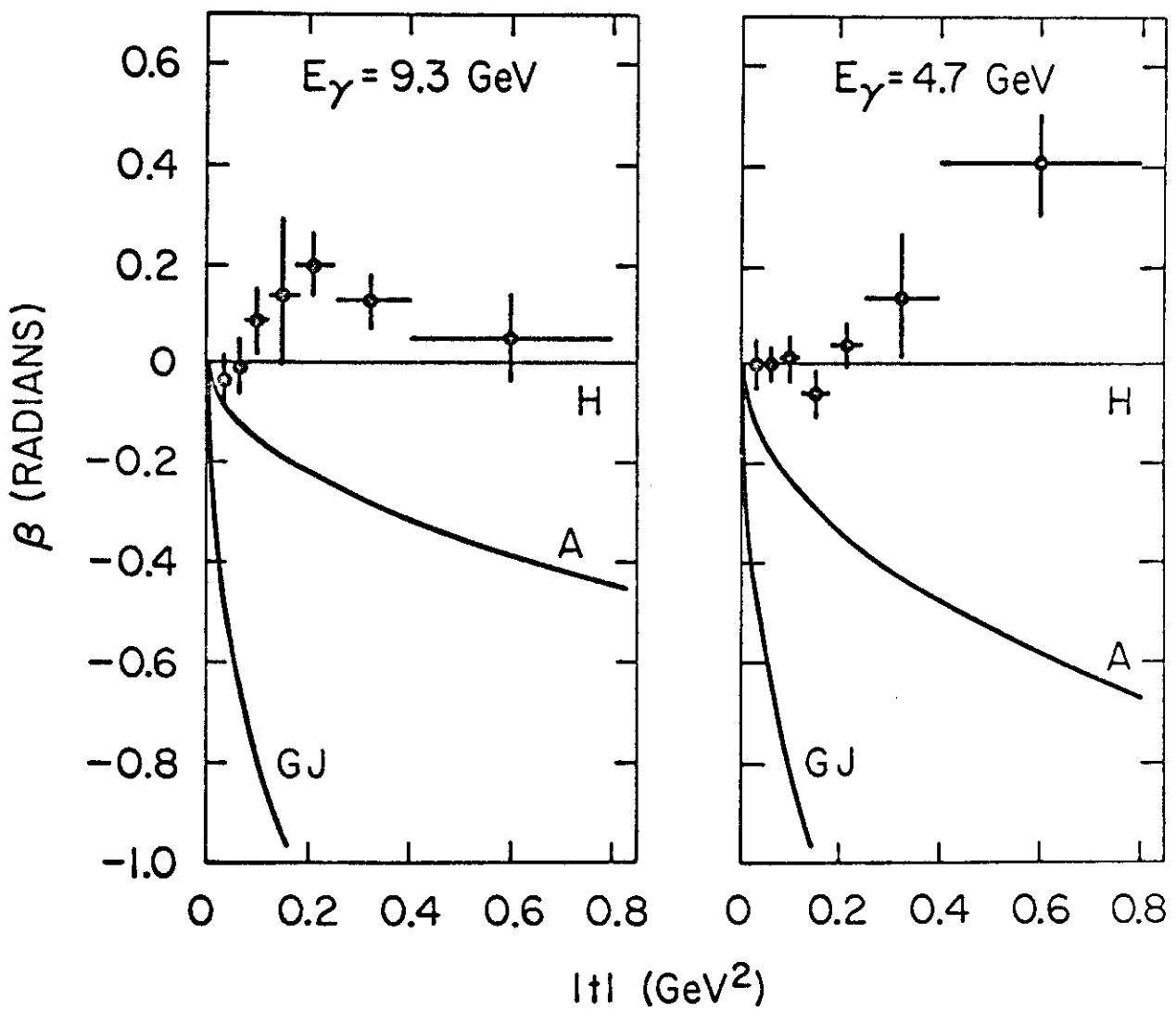


Fig. 4



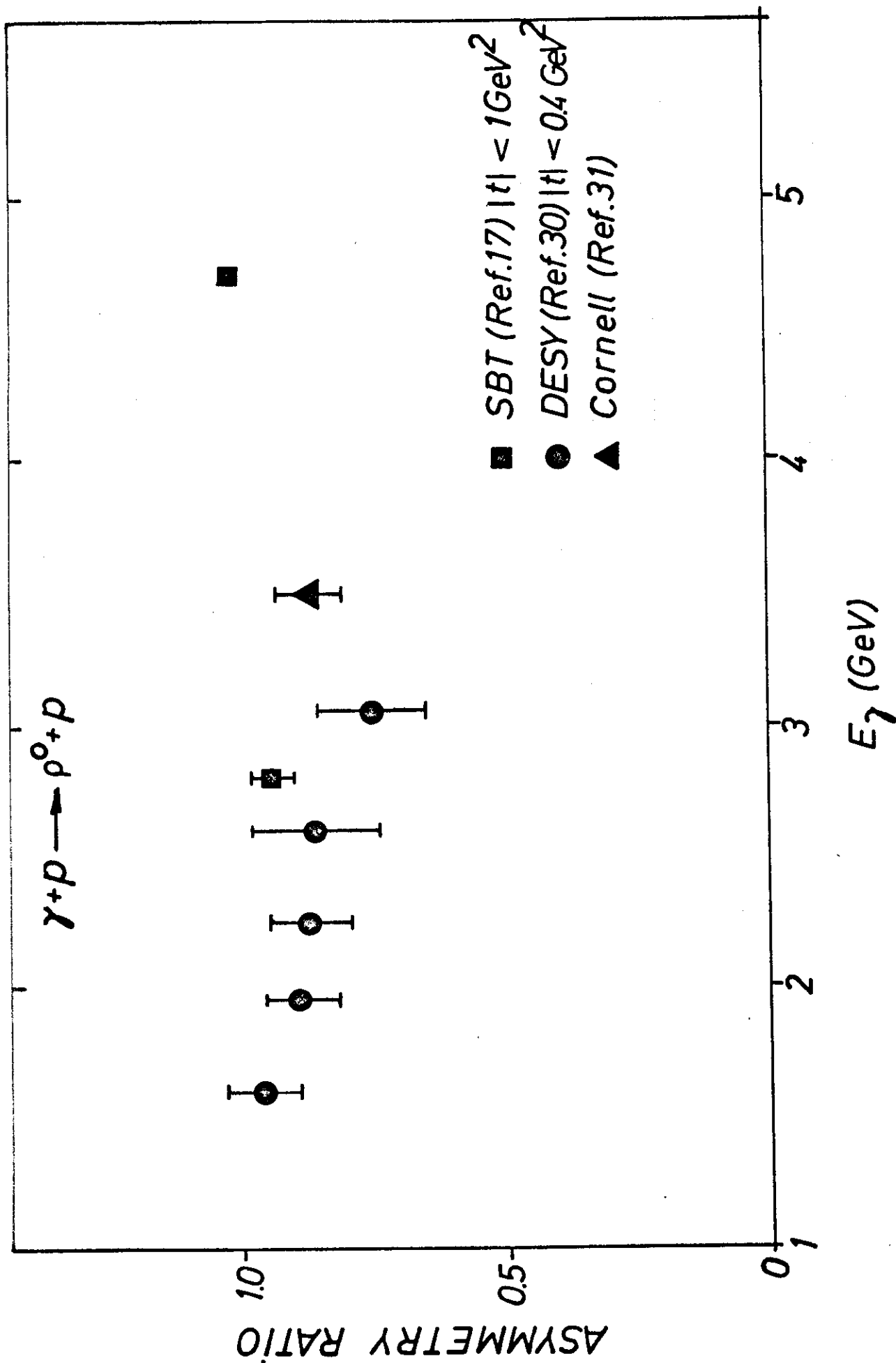


Fig. 5

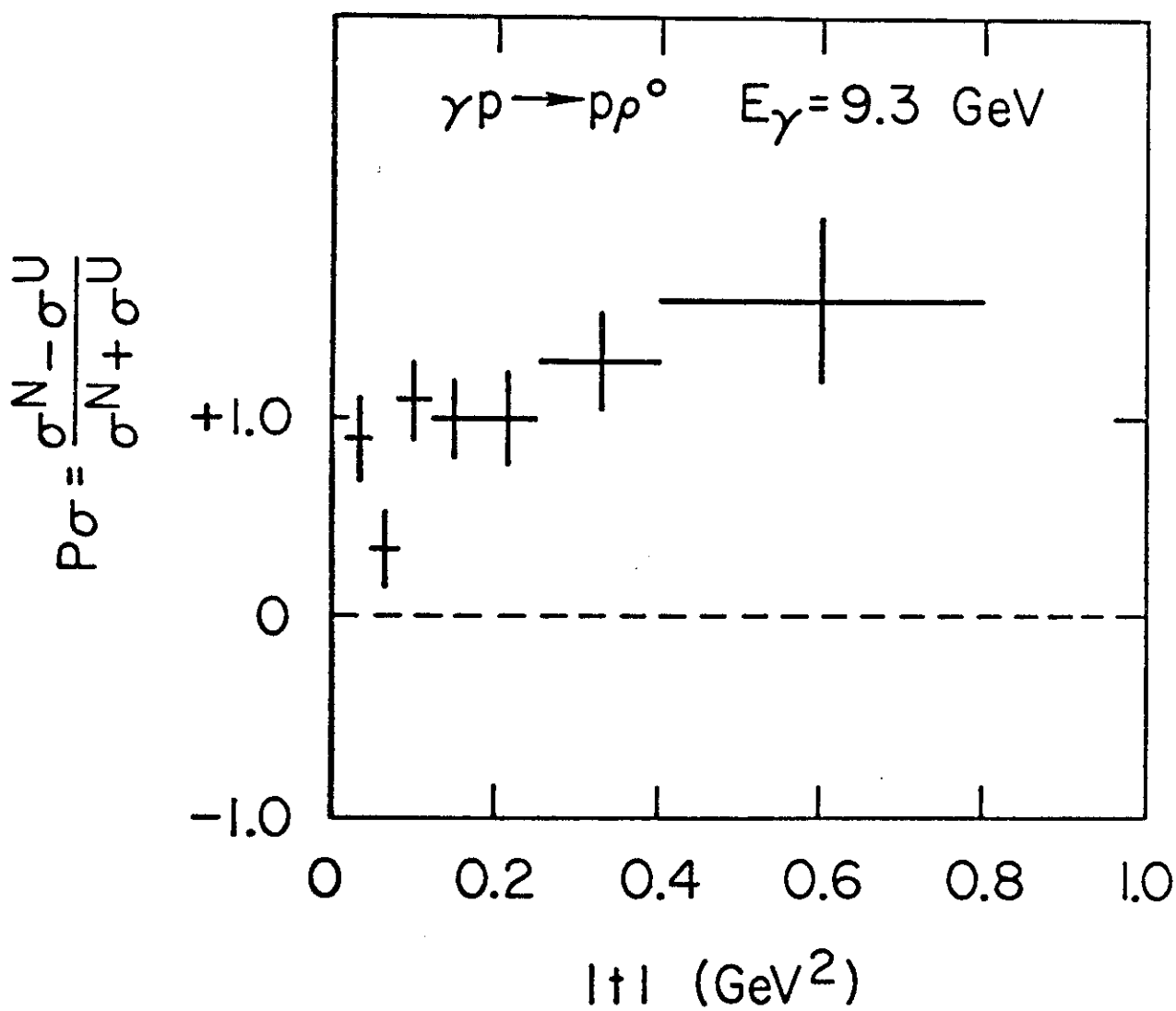
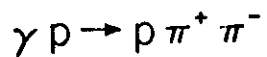


Fig. 6



$E_\gamma = 2.8 \text{ GeV}$

$E_\gamma = 4.7 \text{ GeV}$

$|t| < 0.4 \text{ GeV}^2$

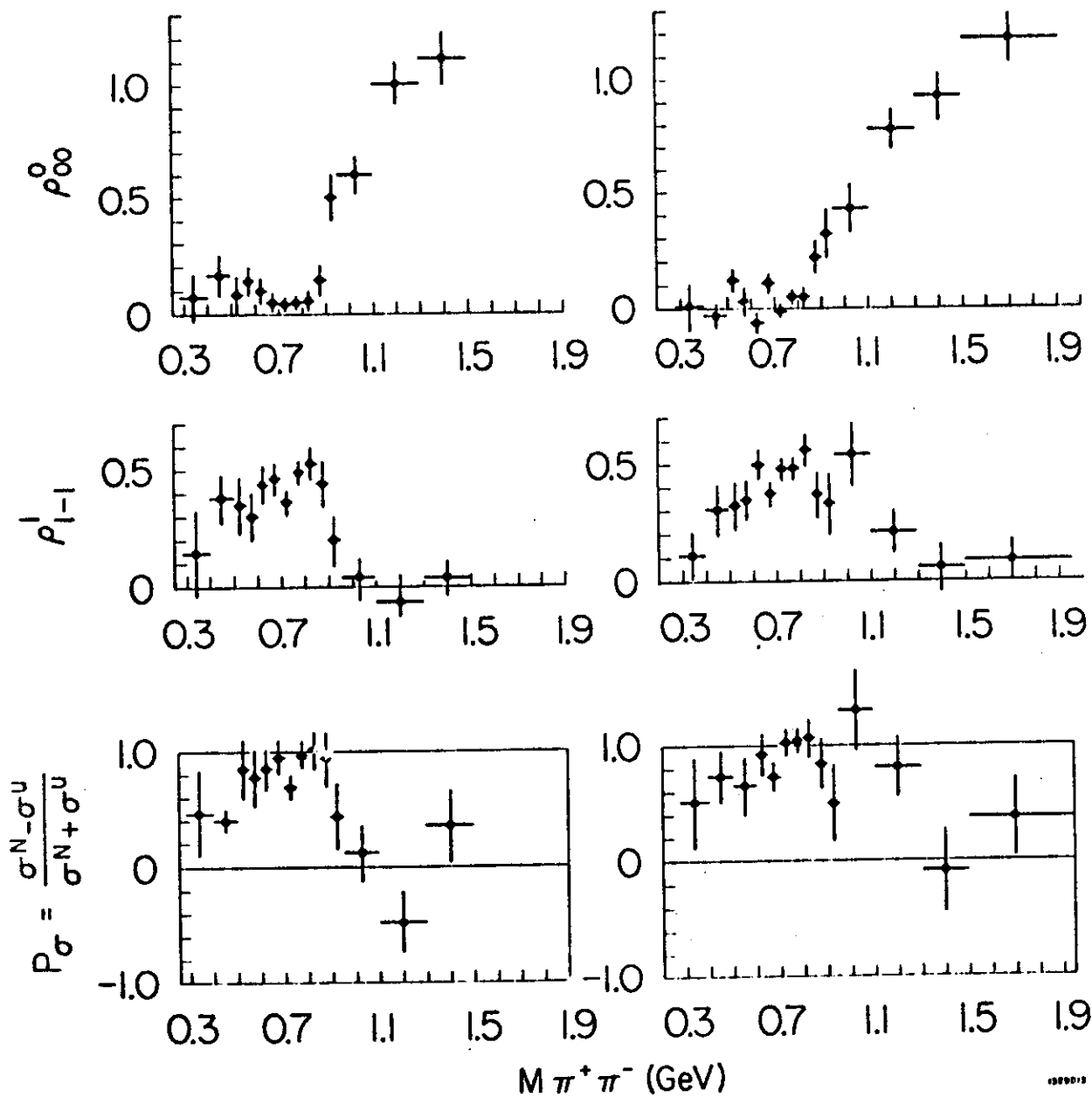
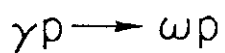
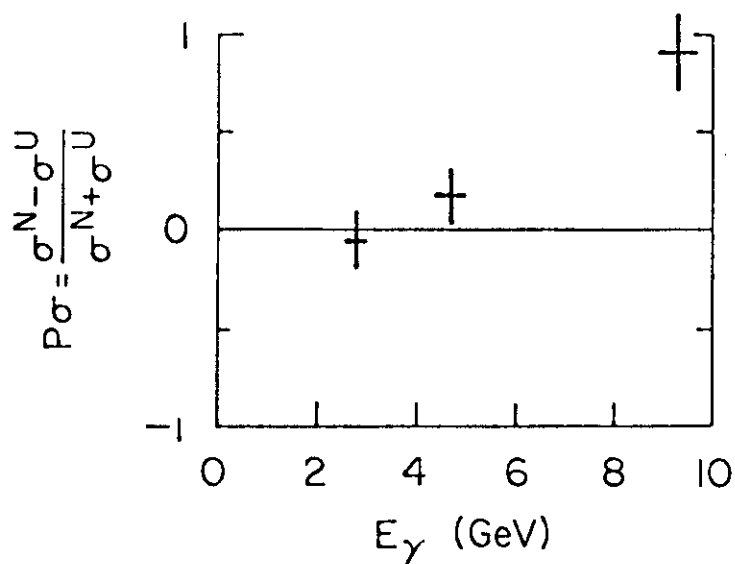
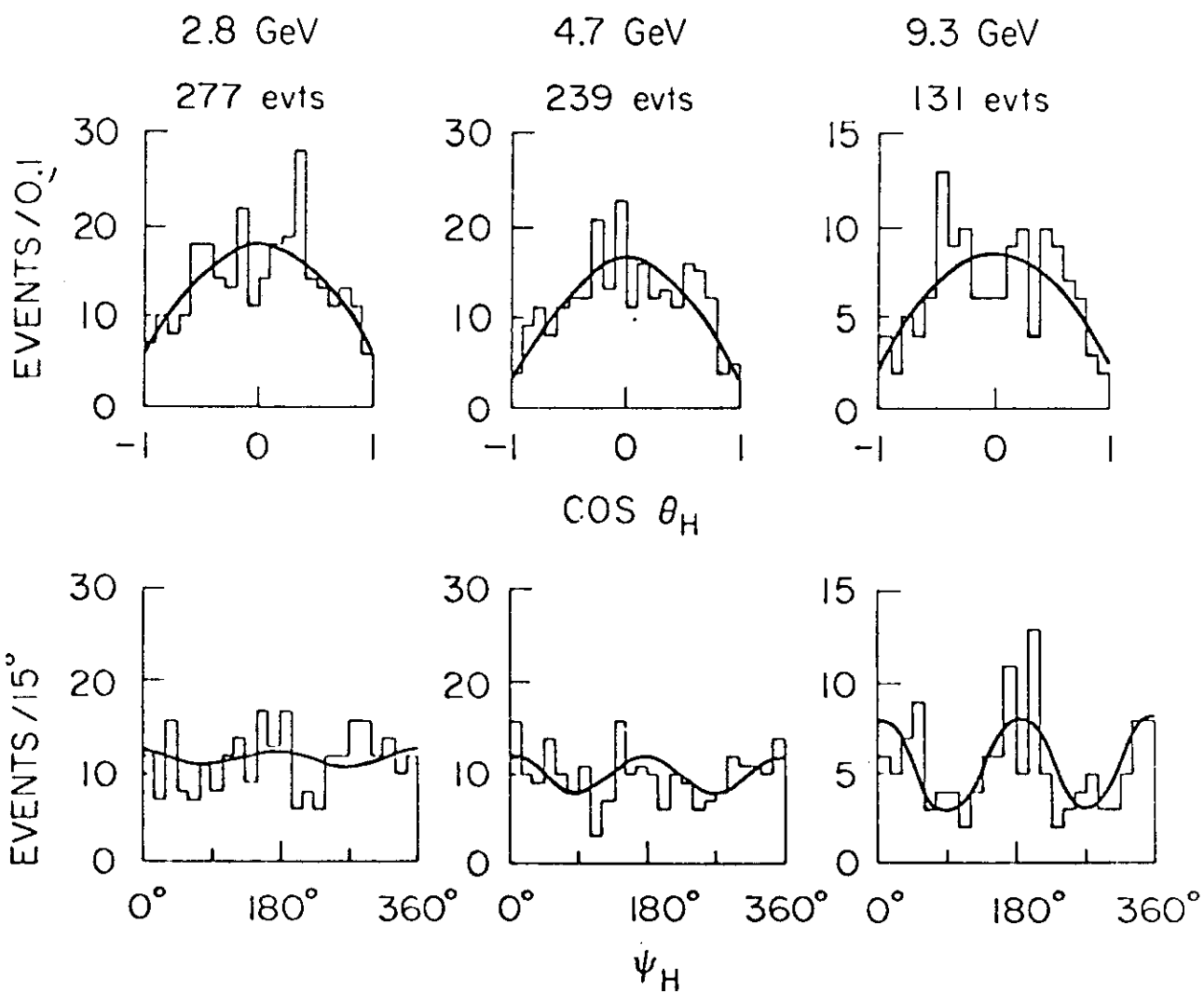


Fig. 7



$$0.02 < |t| < 0.3 \text{ GeV}^2$$



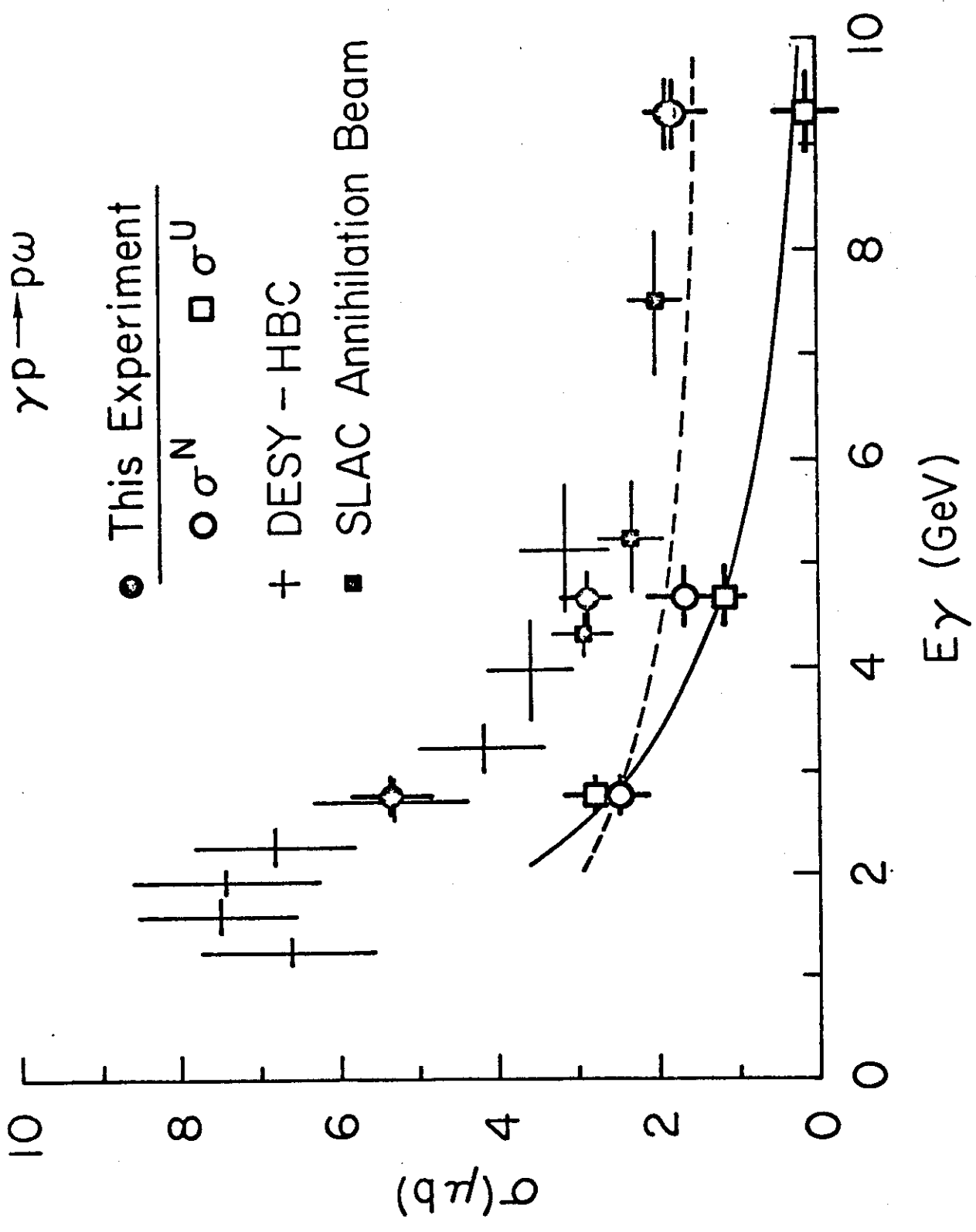
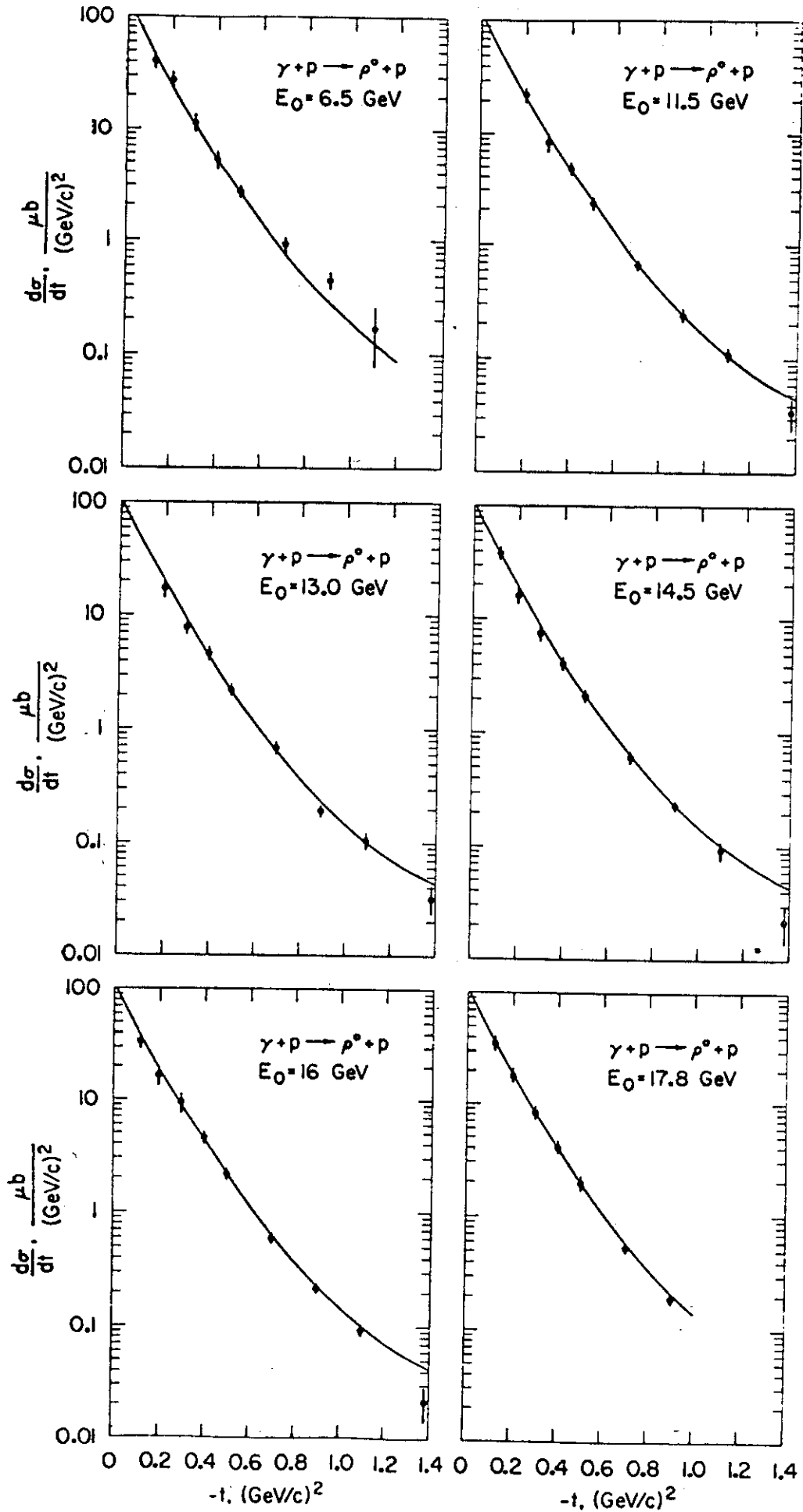


Fig. 9



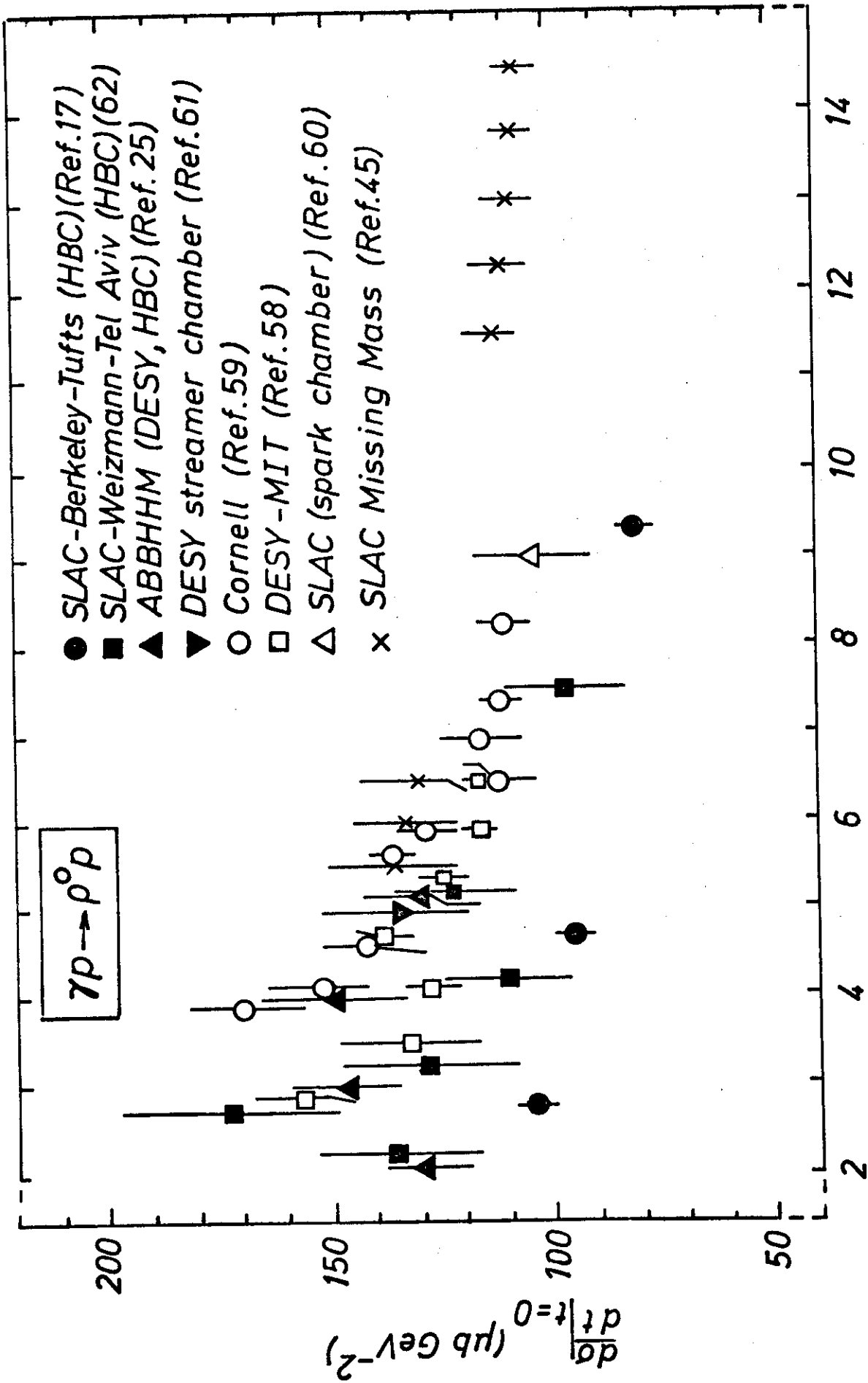


Fig. 11

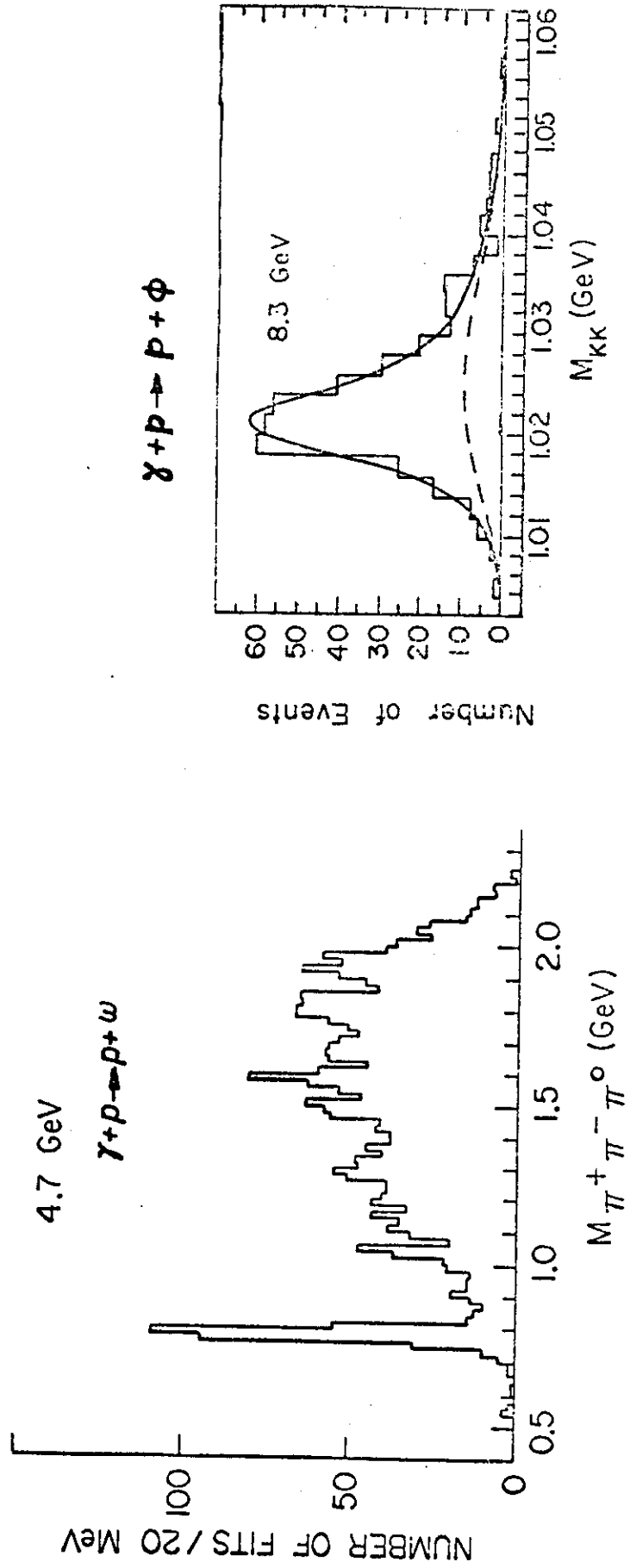
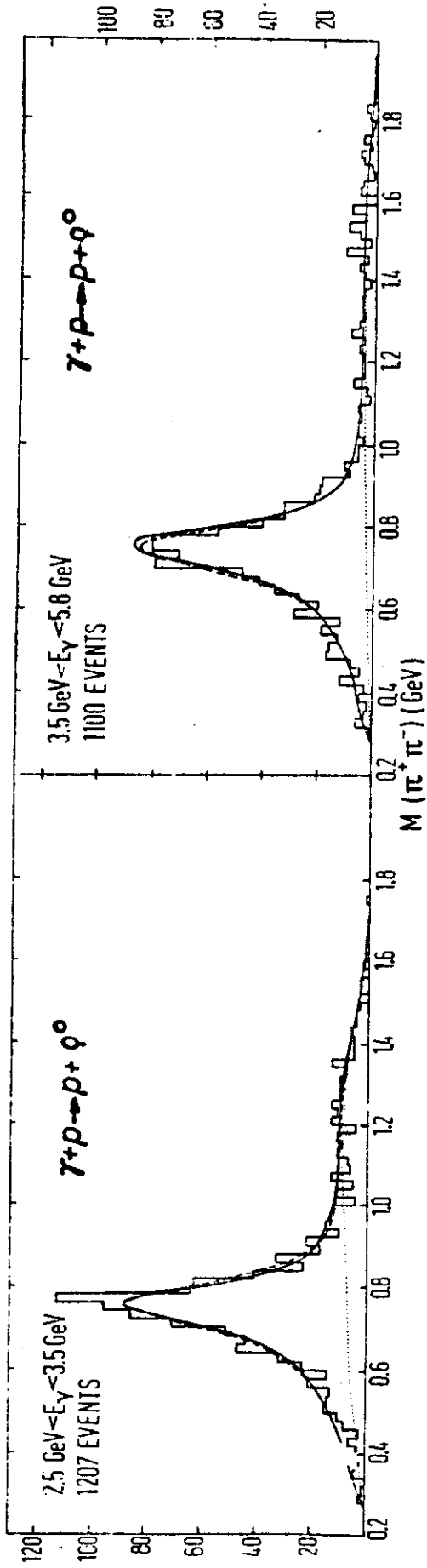


Fig. 12



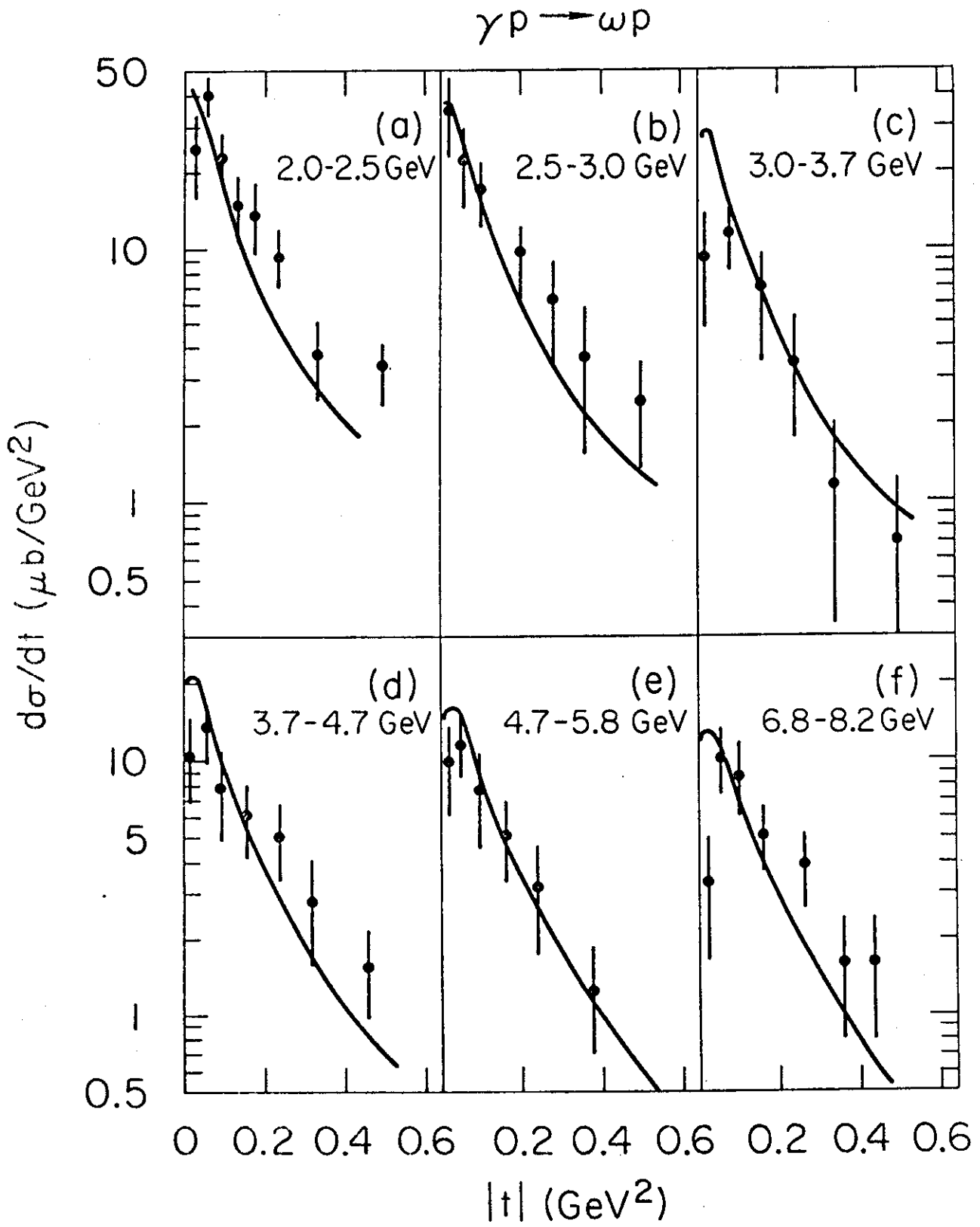


Fig. 13

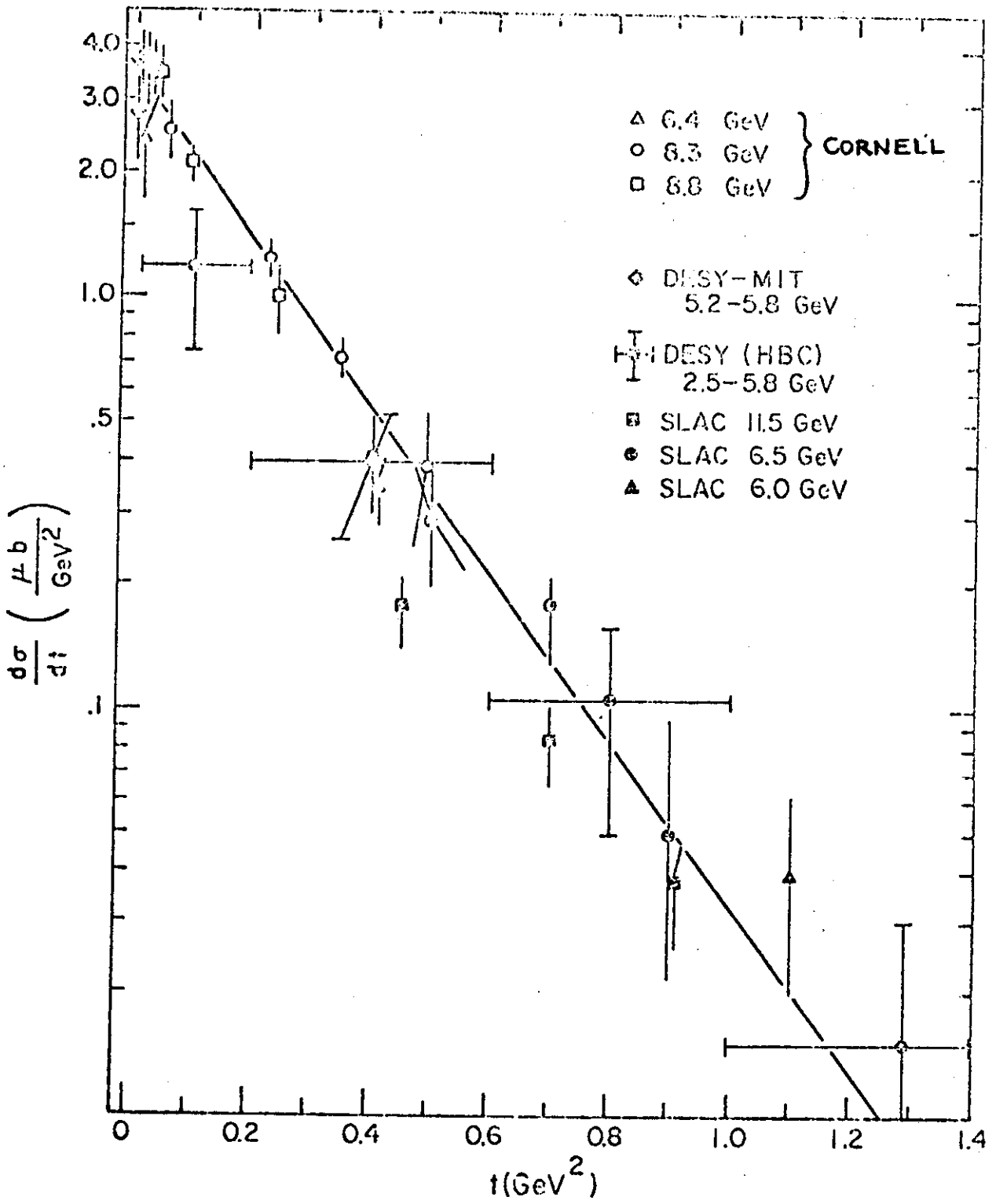


Fig. 14

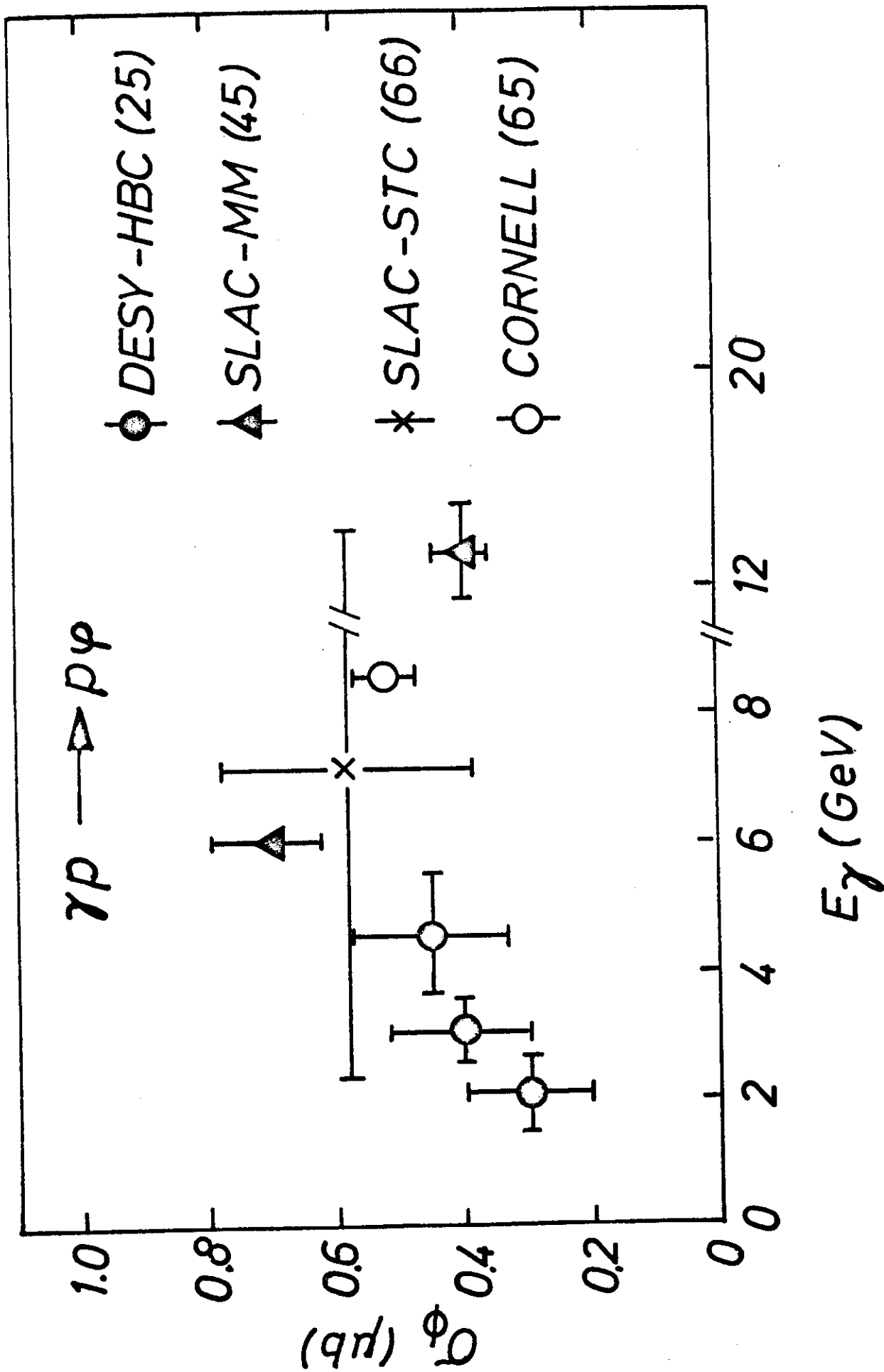


Fig. 15

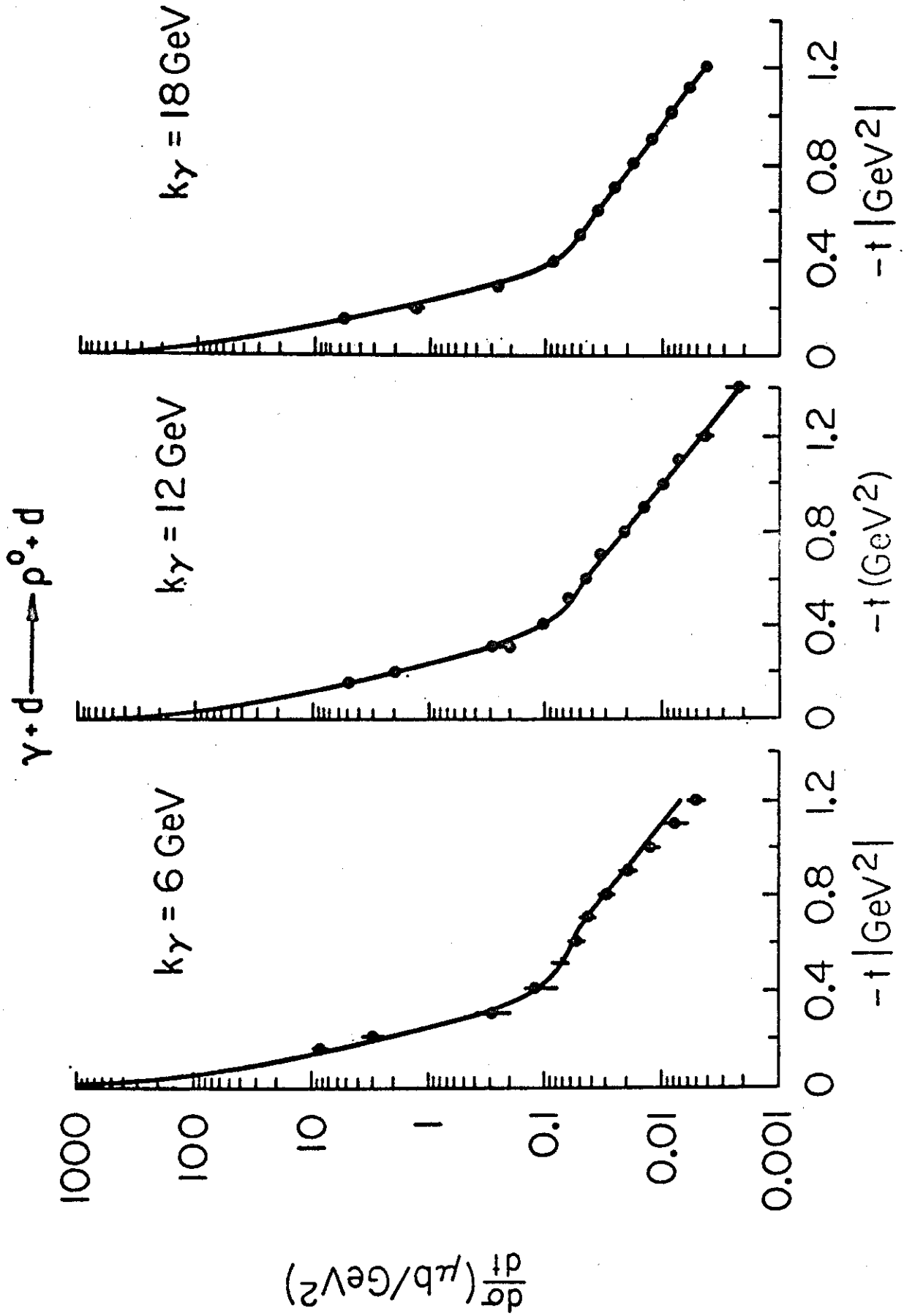


Fig. 16

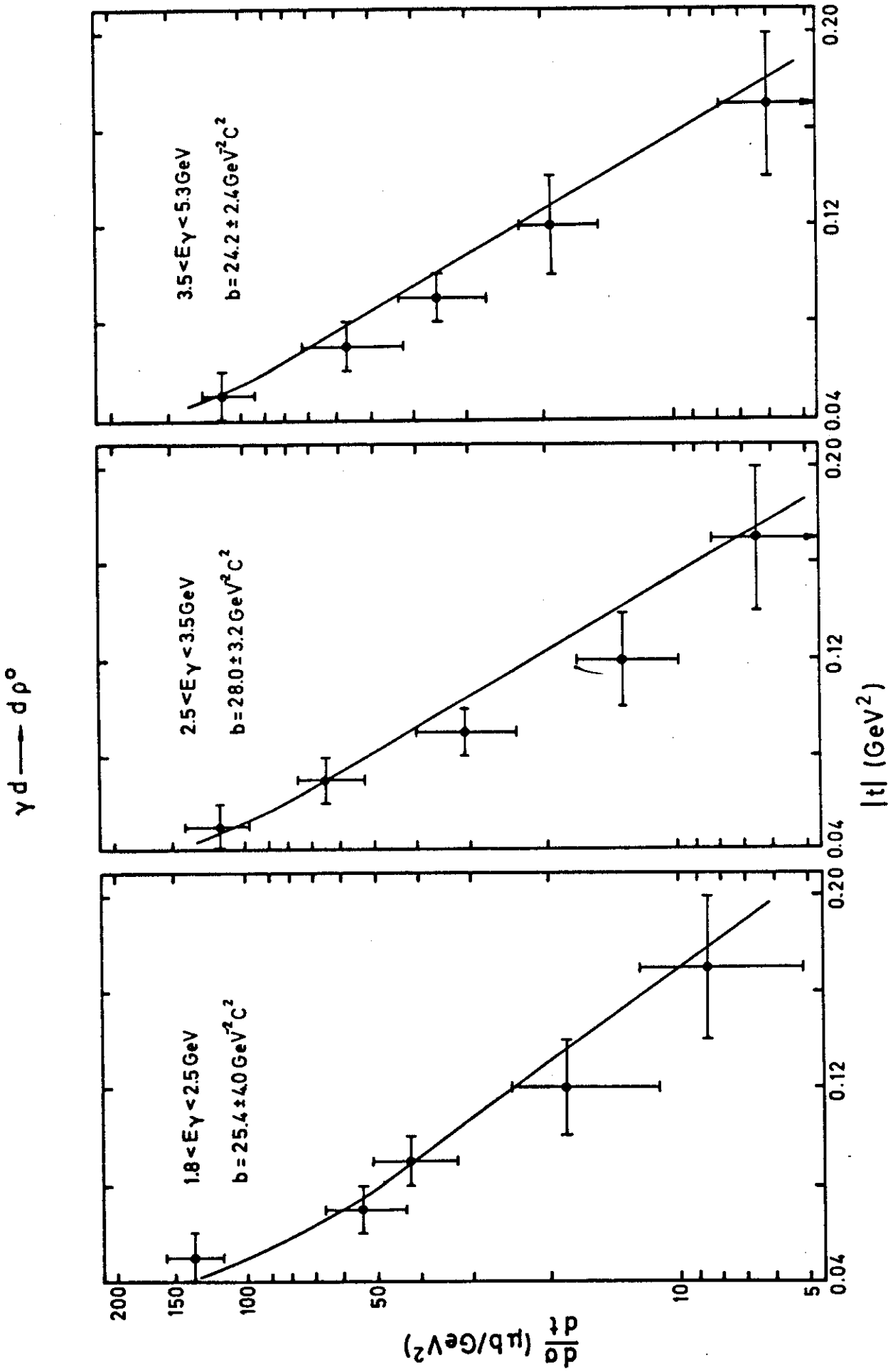


Fig. 17

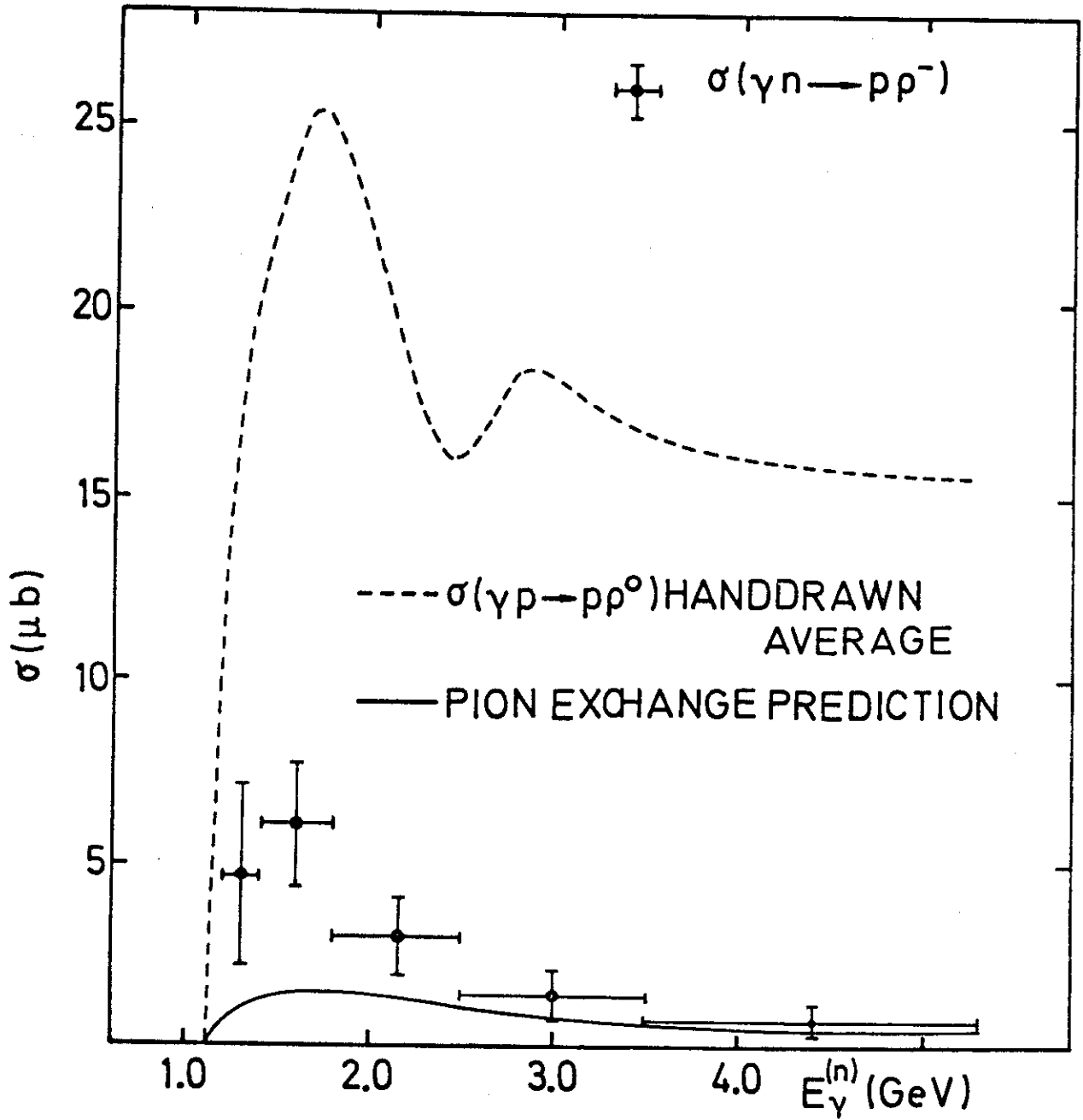


Fig. 18

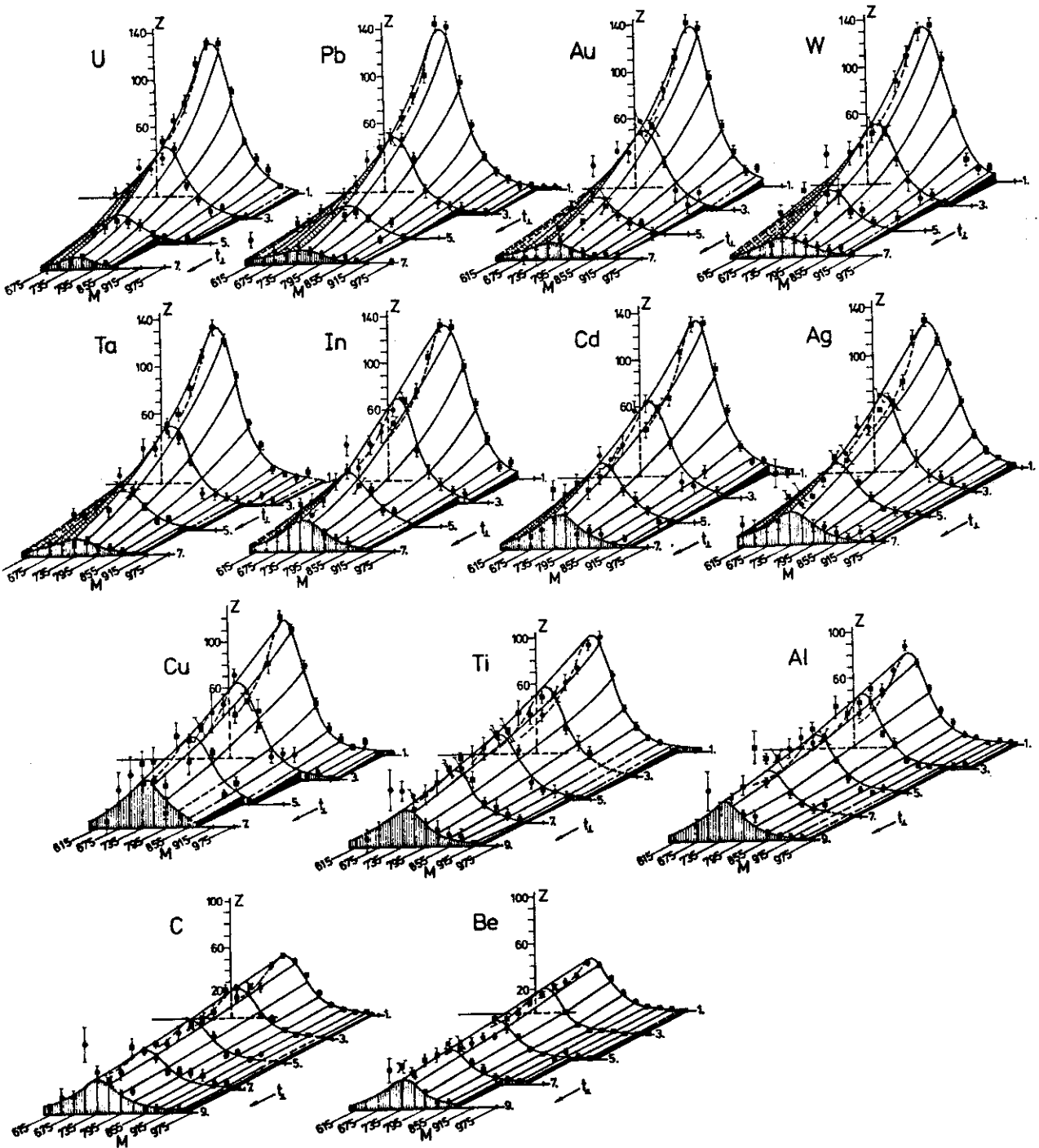


Fig. 19

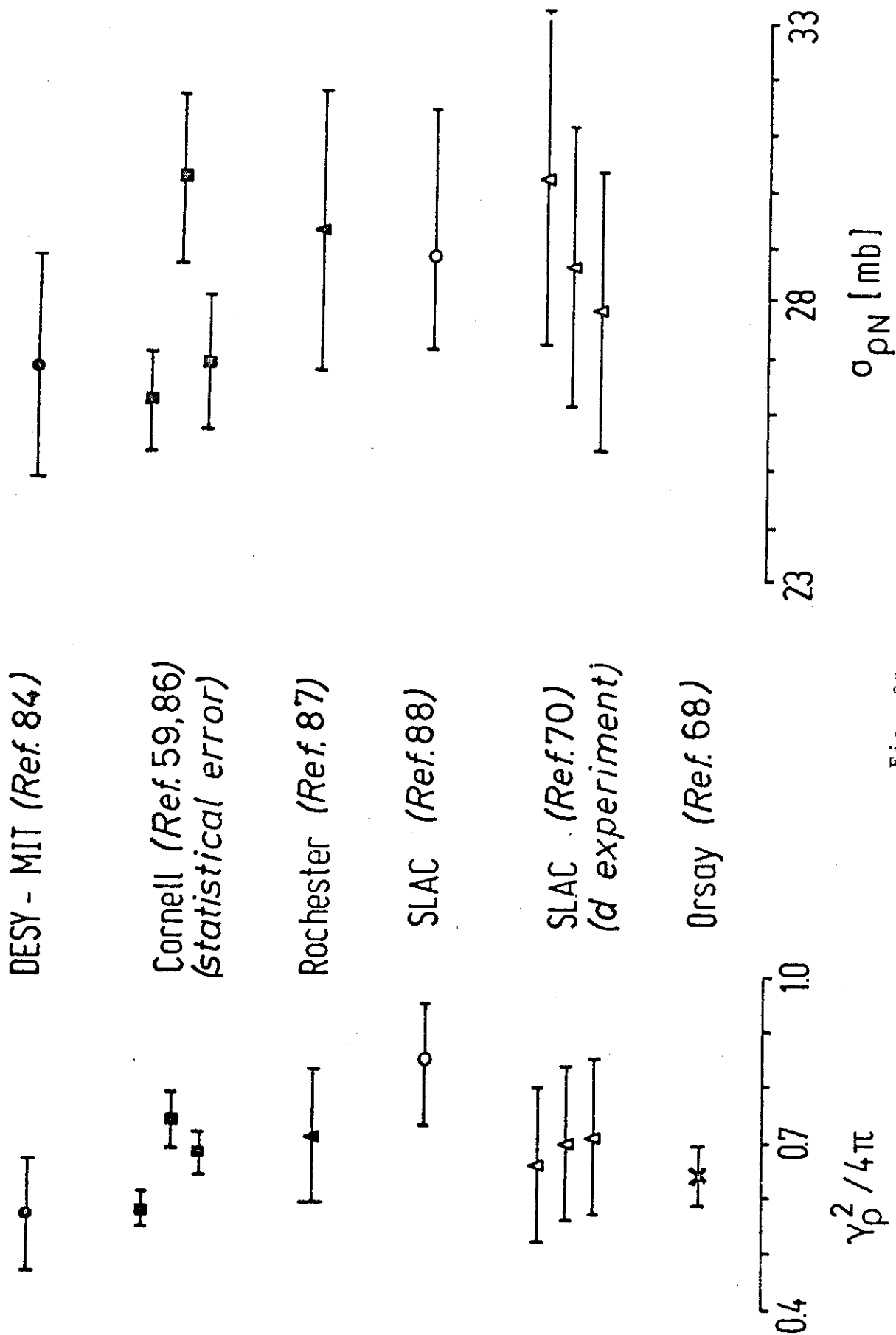


Fig. 20



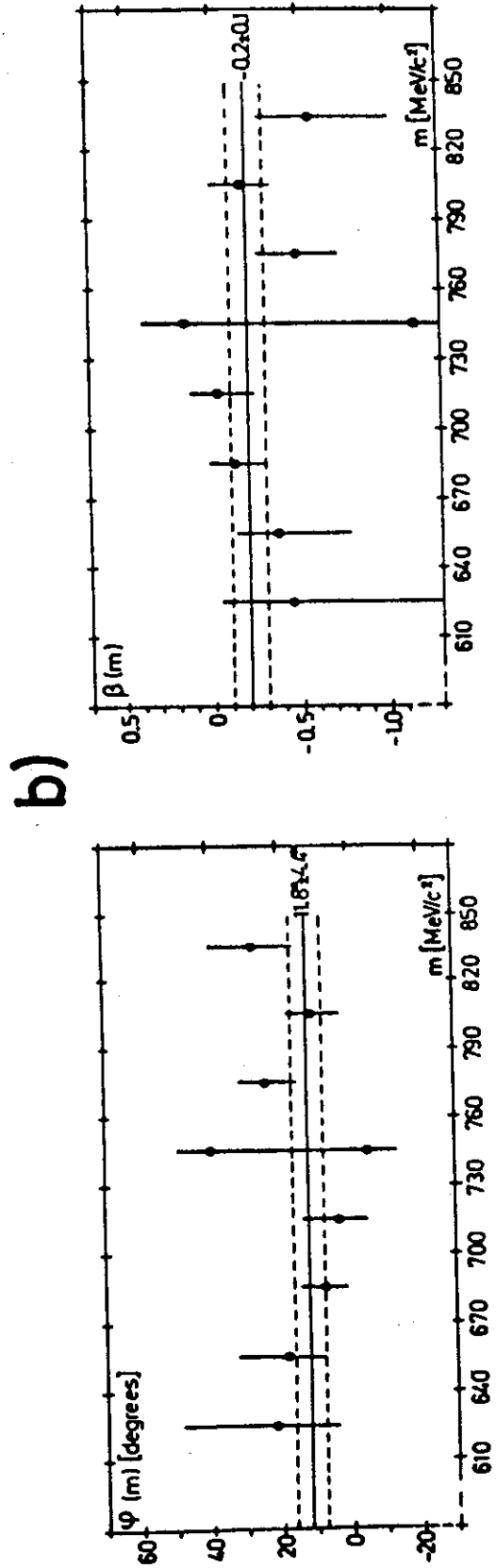
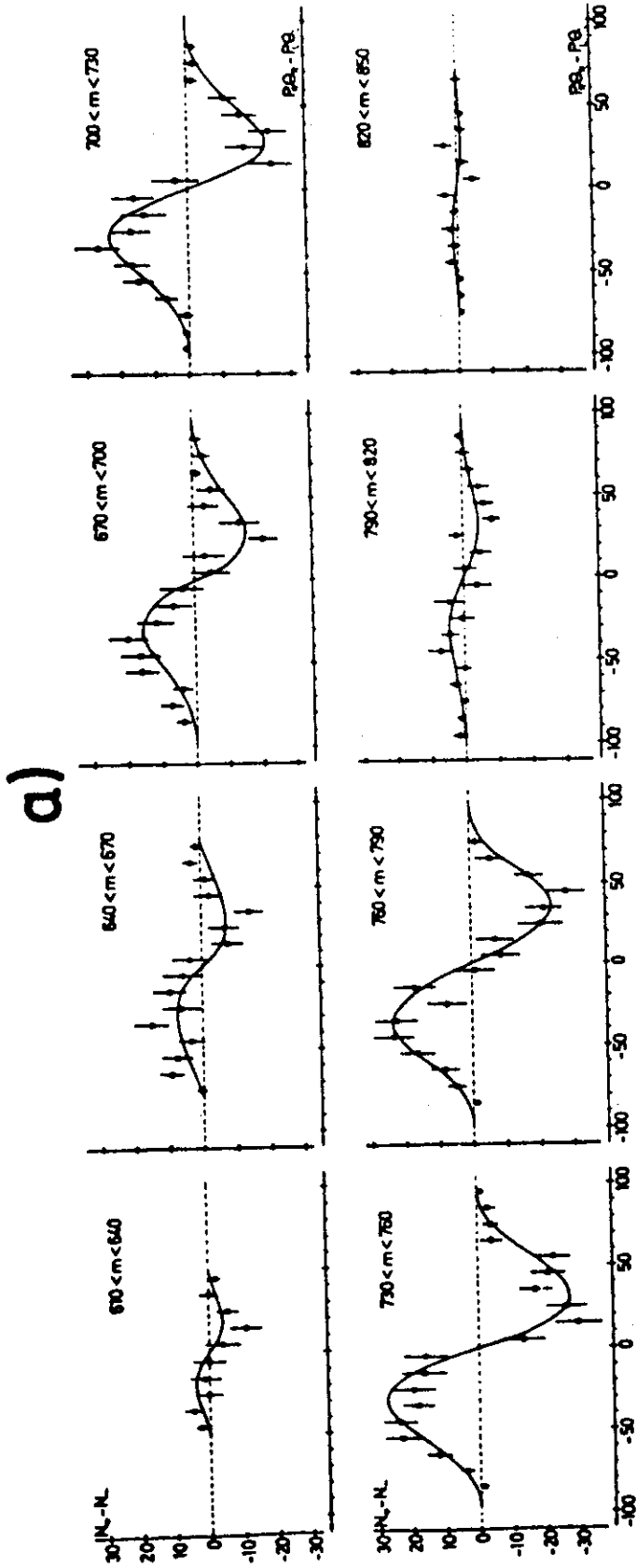


Fig. 21

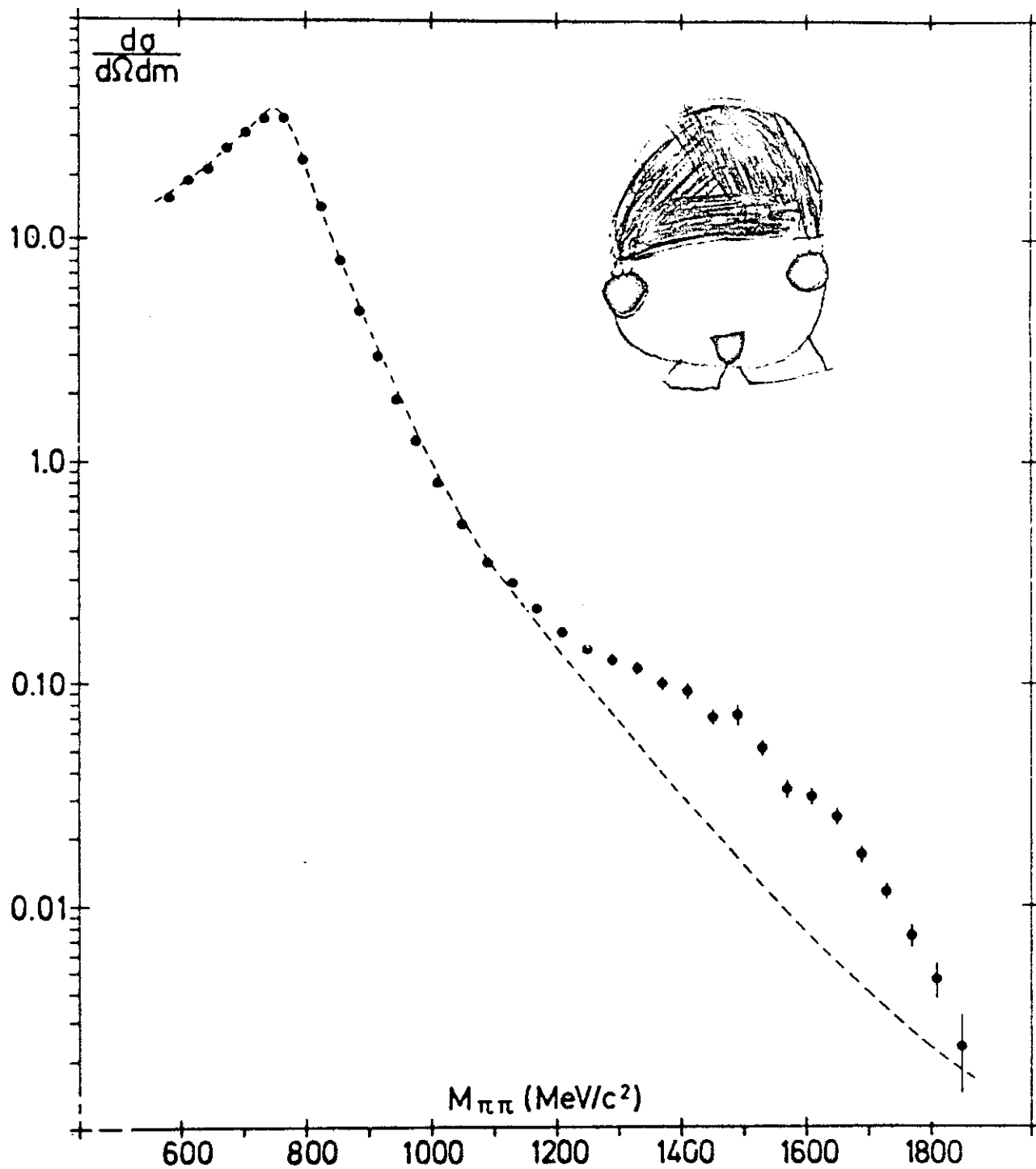


Fig. 22

